Russian Math. Surveys **62**:3 1–26

Uspekhi Mat. Nauk **62**:3 47–72 DOI 10.1070/RM2007v062n03ABEH004411

This paper is dedicated to the memory of Victor Yudovich with whom the author discussed some of these ideas in their early stages

Orthonormal quaternion frames, Lagrangian evolution equations, and the three-dimensional Euler equations

J. D. Gibbon

Abstract. More than 160 years after their invention by Hamilton, quaternions are now widely used in the aerospace and computer animation industries to track the orientation and paths of moving objects undergoing three-axis rotations. Here it is shown that they provide a natural way of selecting an appropriate orthonormal frame — designated the quaternion-frame — for a particle in a Lagrangian flow, and of obtaining the equations for its dynamics. How these ideas can be applied to the three-dimensional Euler fluid equations is then considered. This work has some bearing on the issue of whether the Euler equations develop a singularity in a finite time. Some of the literature on this topic is reviewed, which includes both the Beale–Kato–Majda theorem and associated work on the direction of vorticity by Constantin, Fefferman, and Majda and by Deng, Hou, and Yu. It is then shown how the quaternion formalism provides an alternative formulation in terms of the Hessian of the pressure.

Contents

1. General introduction 2
  1.1. Historical remarks 2
  1.2. Application to fluid dynamics 2
  1.3. Blow-up in the three-dimensional Euler equations 5
  1.4. Definition and properties of quaternions 6
2. Lagrangian evolution equations and an orthonormal frame 8
3. Quaternions and the incompressible $3D$ Euler equations 12
4. The BKM theorem and the direction of vorticity 14
  4.1. The work of Constantin, Fefferman, and Majda 16
  4.2. The work of Deng, Hou, and Yu 17
  4.3. The non-constancy of α_p and $\boldsymbol{\chi}_p$: quaternions and the direction of vorticity 18
5. A final example: the equations of incompressible ideal MHD 20
6. Conclusion 21
Bibliography 23

The material in this review is based on the contents of an invited lecture given at the meeting “Mathematical Hydrodynamics” held at the Steklov Institute Moscow, in June 2006.

AMS 2000 *Mathematics Subject Classification.* Primary 35Q35; Secondary 35B40, 35L60, 35Q30, 46N20, 76B03, 76B47, 76D05, 76F02, 76F05, 76W05.

1. General introduction

1.1. Historical remarks. Everyone loves a good story: William Rowan Hamilton's feverish excitement at the discovery of his famous formula for quaternions on 16th October 1843 as a composition rule for orienting his telescope; his inscription of this formula on Broome (Brougham) Bridge in Dublin; and then his long and eventually unfruitful championing of the role of quaternions in mechanics, are all elements of a story that has lost none of its appeal [1], [2]. Hamilton's name is still revered today for the audacity and depth of his ideas in modern mechanics and what we now call symplectic geometry [3]–[5]. Indeed, evidence of his thinking is everywhere in both classical and quantum mathematical physics and applied mathematics, yet in his own century his work on quaternions evoked criticism and even derision from many influential fellow scientists.[1] Ultimately quaternions lost out to the tensor notation of Gibbs, which is the basis of the 3-vector notation universally used today.

In essence, Hamilton's multiplication rule for quaternions represents compositions of rotations [6]–[11]. This property has been ably exploited in modern inertial guidance systems in the aerospace industry where computing the orientation and the paths of rapidly moving rotating satellites and aircraft is essential. Kuipers' book [12] explains the details of how calculations with quaternions in this field are performed in practice. Just as importantly, the computer graphics community also uses them to determine the orientation of tumbling objects in animations. In his valuable and eminently readable book, Andrew Hanson [2] says in his introduction:

> Although the advantages of the quaternion forms for the basic equations of attitude control — clearly presented in Cayley [6], Hamilton [7], [8], and especially Tait [9] — had been noticed by the aeronautics and astronautics community, the technology did not penetrate the computer animation community until the landmark SIGGRAPH-1985 paper of Shoemake [13]. The importance of Shoemake's paper is that it took the concept of the orientation frame for moving $3D$ objects and cameras, which require precise orientation specification, exposed the deficiencies of the then-standard Euler-angle methods,[2] and introduced quaternions to animators as a solution.

Hamilton's 19th century critics were correct, of course, in asserting that quaternions need 3-vector algebra to manipulate them, yet the use the aero/astronautics and animation communities have made of them are one more illustration of the universally acknowledged truth that while new mathematical tools may not be of immediate use, and may appear to be too abstract or overly elaborate, they may nevertheless turn out to have powerful applications undreamed of at the time of their invention.

1.2. Application to fluid dynamics. The close association of quaternions with rigid body rotations [9]–[11] points to their use in the incompressible Euler equations for an inviscid fluid as a natural language for describing the alignment of vorticity

[1] Kelvin was one such example: see [1].

[2] A well-known deficiency of Euler-angle methods lies in the problems they suffer at the poles of the sphere where the azimuthal angle is not defined.

with the eigenvectors of the strain rate that are responsible for its non-linear evolution. For a three-dimensional fluid velocity field $\boldsymbol{u}(\boldsymbol{x},t)$ with pressure $p(\boldsymbol{x},t)$, the incompressible Euler equations are [14]–[18]

$$\frac{D\boldsymbol{u}}{Dt} = -\nabla p, \tag{1.1}$$

where the material (substantial) derivative is defined by

$$\frac{D}{Dt} = \frac{\partial}{\partial t} + \boldsymbol{u}\cdot\nabla. \tag{1.2}$$

The motion is constrained by the incompressibility condition $\operatorname{div}\boldsymbol{u} = 0$. The crucial dynamics lies in the evolution of the velocity gradient matrix $\nabla\boldsymbol{u} = \{u_{i,j}\}$ which comes from the differentiation of (1.1),

$$\frac{Du_{i,j}}{Dt} = -u_{i,k}u_{k,j} - P_{ij}, \tag{1.3}$$

where P_{ij} is the Hessian matrix of the pressure,

$$P_{ij} = \frac{\partial^2 p}{\partial x_i\,\partial x_j}. \tag{1.4}$$

The incompressibility condition $\operatorname{div}\boldsymbol{u} = 0$ insists that $\operatorname{Tr} u_{i,j} = 0$ which, when applied to (1.3), gives

$$\operatorname{Tr} P = \Delta p = -u_{i,k}u_{k,i} = \frac{1}{2}\boldsymbol{\omega}^2 - \operatorname{Tr} S^2. \tag{1.5}$$

In (1.5) above, $\boldsymbol{\omega}$ is the vorticity and S is the strain matrix, whose elements are defined by

$$S_{ij} = \frac{1}{2}(u_{i,j} + u_{j,i}). \tag{1.6}$$

This is a symmetric matrix, the alignment of whose eigenvectors $\boldsymbol{e}_i$ is fundamental to the dynamics of the Euler equations. For instance, vortex tubes and sheets (Burgers' vortices and shear layers) always have one eigenvector aligned with the vorticity vector $\boldsymbol{\omega}$ [18].

This review cannot hope to deal with every aspect of the three-dimensional Euler equations. Here we concentrate on one particular aspect, which is the role played by quaternions in providing a natural language for extracting geometric information from the evolution of $u_{i,j}$. Because they are particularly effective in computing the orientation of rotating objects moving in three-dimensional paths they might be useful in understanding how general Lagrangian flows behave, particularly in finding the evolution of the orthonormal frame of particles moving in such a flow. These particles could be of the passive tracer type transported by a background flow or they could be Lagrangian fluid parcels. Recent experiments in turbulent flows can now detect the trajectories of tracer particles at high Reynolds numbers [19]–[28]: see [19], Fig. 1. For any system involving a path represented as a three-dimensional space-curve, the usual practice is to consider the Frenet-frame of a trajectory constituted by the unit tangent vector, the normal, and the bi-normal [2], [28]. In navigational language, this represents the corkscrew-like pitch, yaw, and roll of the motion. While the Frenet-frame describes the path, it ignores the dynamics that generates the motion. Attempts have been made in this direction using the eigenvectors $\boldsymbol{e}_i$ of S but ran into difficulties because the equations of motion for $\boldsymbol{e}_i$ are unknown [29]. In § 2 another orthonormal frame is introduced that is associated with the motion of each Lagrangian particle. It is designated the *quaternion-frame*: this frame may be envisioned as moving with the Lagrangian particles but its evolution derives from the Eulerian equations of motion. The advantage of this approach lies in the fact that the Lagrangian dynamics of the quaternion-frame can be connected to the fluid motion through the pressure Hessian P defined in (1.4).

Let us now consider a general picture of a Lagrangian flow system of equations. Suppose that $\boldsymbol{w}$ is a contravariant vector quantity attached to a particle following a flow along characteristic paths $d\boldsymbol{x}/dt = \boldsymbol{u}(\boldsymbol{x}, t)$ of a velocity field $\boldsymbol{u}$. Let us consider the abstract Lagrangian flow equation

$$\frac{D\boldsymbol{w}}{Dt} = \boldsymbol{a}(\boldsymbol{x}, t), \qquad \frac{D}{Dt} = \frac{\partial}{\partial t} + \boldsymbol{u}\cdot\nabla, \tag{1.7}$$

where the material derivative has its standard definition, and in turn, $\boldsymbol{a}$ satisfies the Lagrangian equation

$$\frac{D^2\boldsymbol{w}}{Dt^2} = \frac{D\boldsymbol{a}}{Dt} = \boldsymbol{b}(\boldsymbol{x}, t). \tag{1.8}$$

So far, these are just kinematic rates of change following the characteristics of the velocity generating the path $\boldsymbol{x}(t)$ determined from $d\boldsymbol{x}/dt = \boldsymbol{u}(\boldsymbol{x}, t)$. Examples of systems that (1.7) might represent are as follows.

1. If $\boldsymbol{w}$ represents the vorticity $\boldsymbol{\omega} = \operatorname{curl}\boldsymbol{u}$ of the incompressible Euler fluid equations, then $\boldsymbol{a} = \boldsymbol{\omega}\cdot\nabla\boldsymbol{u}$ and $\operatorname{div}\boldsymbol{u} = 0$. With rotation $\boldsymbol{w}$ would be $\boldsymbol{w} \equiv \widetilde{\boldsymbol{\omega}} = \rho_0^{-1}(\boldsymbol{\omega} + 2\boldsymbol{\Omega})$.
2. For the barotropic compressible Euler fluid equations (where the pressure $p = p(\rho)$ is density dependent only) $\boldsymbol{w} \equiv \boldsymbol{\omega}_{\boldsymbol{\rho}} = \rho^{-1}\boldsymbol{\omega}$, in which case $\boldsymbol{a} = \boldsymbol{\omega}_{\boldsymbol{\rho}}\cdot\nabla\boldsymbol{u}$ and $\operatorname{div}\boldsymbol{u} = 0$.
3. The vector $\boldsymbol{w}$ could also represent a small vectorial line element $\boldsymbol{\delta\ell}$ that is mixed and stretched by a background flow $\boldsymbol{u}$, in which case $\boldsymbol{a} = \boldsymbol{\delta\ell}\cdot\nabla\boldsymbol{u}$. For example, following Moffatt's analogy between the magnetic field $\boldsymbol{B}$ in ideal incompressible MHD (magnetic hydrodynamics) and vorticity [30], if $\boldsymbol{w}$ is chosen such that $\boldsymbol{w} \equiv \boldsymbol{B}$, then $\boldsymbol{a} = \boldsymbol{B}\cdot\nabla\boldsymbol{u}$ with $\operatorname{div}\boldsymbol{B} = 0$. In a more generalized form, the vector $\boldsymbol{w}$ could also represent the Elsasser variables $\boldsymbol{w}^{\pm} = \boldsymbol{u} \pm \boldsymbol{B}$, in which case $\boldsymbol{a}^{\pm} = \boldsymbol{w}^{\pm}\cdot\nabla\boldsymbol{u}$ with two material derivatives.
4. The semigeostrophic (SG) model used in atmospheric physics can also be cast in the form of (1.7); for instance, one could choose $\boldsymbol{w} = \boldsymbol{x}$, $\boldsymbol{a} = \boldsymbol{u}$, and $\boldsymbol{b}$ is computed from the SG-model through the semigeostrophic and ageostrophic contributions [31]–[33].
5. For a passive tracer particle with velocity $\boldsymbol{w}$ in a fluid transported by a background velocity field $\boldsymbol{u}$, the particle's acceleration would be $\boldsymbol{a}$ (see [34], [16]).

In cases 1–3 above, if $\boldsymbol{w}$ satisfies the standard Eulerian form

$$\frac{D\boldsymbol{w}}{Dt} = \boldsymbol{w}\cdot\nabla\boldsymbol{u}, \tag{1.9}$$

then to find $\boldsymbol{b}$ it follows from Ertel's theorem (see [35]) that

$$\frac{D(\boldsymbol{w}\cdot\nabla\boldsymbol{\mu})}{Dt} = \boldsymbol{w}\cdot\nabla\left(\frac{D\boldsymbol{\mu}}{Dt}\right), \tag{1.10}$$

which means that the operators D/Dt and $\boldsymbol{w}\cdot\nabla$ commute for any differentiable function $\boldsymbol{\mu}(\boldsymbol{x},t)$. Choosing $\boldsymbol{\mu}=\boldsymbol{u}$ as in [36], and identifying the flow acceleration as $\boldsymbol{Q}(\boldsymbol{x},t)$ so that $D\boldsymbol{u}/Dt=\boldsymbol{Q}(\boldsymbol{x},t)$, we have

$$\frac{D^2\boldsymbol{w}}{Dt^2} = \boldsymbol{w}\cdot\nabla\left(\frac{D\boldsymbol{u}}{Dt}\right) = \boldsymbol{w}\cdot\nabla\boldsymbol{Q}. \tag{1.11}$$

In each of the cases 1–3 above, $\boldsymbol{Q}$ is readily identifiable, and thus we have $\boldsymbol{b}$:

$$\frac{D\boldsymbol{a}}{Dt} = \boldsymbol{w}\cdot\nabla\boldsymbol{Q} =: \boldsymbol{b}(\boldsymbol{x},t), \tag{1.12}$$

thereby completing the quartet of vectors $(\boldsymbol{u},\boldsymbol{w},\boldsymbol{a},\boldsymbol{b})$. In § 2 it will be shown that knowledge of the quartet of vectors $(\boldsymbol{u},\boldsymbol{w},\boldsymbol{a},\boldsymbol{b})$ determines the *quaternion-frame*, which is a completely natural orthonormal frame for the Lagrangian dynamics. Modulo a rotation around $\boldsymbol{w}$, the quaternion-frame turns out to be the Frenet-frame attached to characteristic curves $\boldsymbol{w}$. Although usually credited to Ertel [35], the result in (1.10), which involves cancellation of non-linear terms of order $O(|\boldsymbol{w}|\,|\nabla\boldsymbol{u}|^2)$, actually goes much further back in the literature than this; see [36]–[40]. While Ertel's theorem above enables us to find a $\boldsymbol{b}$ as in cases 1–3, $\boldsymbol{b}$ must be determined by other means in case 4.

1.3. Blow-up in the three-dimensional Euler equations. The general picture of Lagrangian evolution and the associated quaternion frame is given in § 2. Thereafter this paper will focus on the three-dimensional incompressible Euler equations (1.1) (see § 3) and the global existence of solutions (see § 4).

Many generations of mathematicians could testify to the deceptive simplicity of the Euler equations. The work of the late V. Yudovich [41], who proved the existence and uniqueness of weak solutions of the two-dimensional Euler equations with $\boldsymbol{\omega}_0\in L^\infty$ on unbounded domains, will be remembered as a milestone in Euler dynamics. In the three-dimensional case, while many special solutions are known in terms of simple functions [16]–[18], weak Leray-type solutions with L^2 initial data are unknown. This contrasts with known results for the two-dimensional case on weak and distributional solutions concerning the vortex sheet problem (see Majda and Bertozzi [15]). One of the great open problems in applied mathematics today is whether the three-dimensional Euler equations develop a singularity in a finite time. In physical terms, singular behaviour could potentially occur if a vortex is resolvable only by length scales decreasing to zero in a finite time. While a review of certain aspects of the three-dimensional Euler singularity problem will form part of the later sections of this review, the regularity problem for the Navier–Stokes equations will not be considered; the interested reader should consult [42]–[44].

In the first demonstrable case of Euler blow-up, Stuart [45]–[47] considered solutions of the three-dimensional Euler equations that had linear dependence in two variables x and z; the resulting differential equations in the remaining independent variables y and t displayed finite time singular behaviour. Stuart then showed how the method of characteristics leads to the construction of a complete class of singular solutions [45]. This type of singularity has infinite energy, because the solution is linearly stretched in the both the x and z directions. In a similar fashion, Gibbon, Fokas, and Doering [48] considered another class of infinite-energy solutions whose third component of velocity is linear in z, so that the velocity field takes the form $\boldsymbol{u} = \{u_1(x,y,t), u_2(x,y,t), z\gamma(x,y,t)\}$. These generalize the Burgers' vortex [18] and represent tube- and ring-like structures depending on the sign of $\gamma(x,y,t)$. Strong numerical evidence of singular behaviour on a periodic cross-section found by Ohkitani and Gibbon [49] was confirmed by an analytical proof of blow-up by Constantin [50]. Subsequently, Gibbon, Moore, and Stuart [51] found two explicit singular solutions using the methods outlined in [45].

The Beale–Kato–Majda (BKM) theorem [52] has been the main cornerstone of the analysis of potential *finite-energy* Euler singularities: one version of this theorem is that $\|\boldsymbol{\omega}\|_\infty$ must satisfy (see § 4 for a more precise statement)

$$\int_0^T \|\boldsymbol{\omega}\|_\infty \, d\tau < \infty \tag{1.13}$$

for a global solution to exist up to time T. The most important feature of (1.13) is that it is a single, simple criterion which is easily monitored.

Several refinements of the BKM theorem exist in addition to those by Ponce [53], who replaced $\|\boldsymbol{\omega}\|_\infty$ by $\|S\|_\infty$, and the BMO-version proved by Kozono and Taniuchi [54]. In particular, these take account of the direction in which vorticity grows. The work of Constantin [55] and of Constantin, Fefferman, and Majda [56], reviewed in § 4.1, deserves specific mention. They were the first to make a precise mathematical formulation of how the misalignment of vortex lines might lead to (or prevent) a singularity. This approach and its variants lays the mathematical foundation for the next generation of computational experiments on the Euler equations. § 4.2 is devoted to a review of the work of Deng, Hou, and Yu [57], [58], who have established different criteria on vortex lines. In § 4.3 quaternions are considered as an alternative way of looking at the direction of vorticity [59], which provides us with a different direction-of-vorticity theorem, based on the Hessian matrix of the pressure (1.4). Further discussion and references are left to § 4.

1.4. Definition and properties of quaternions. In terms of any scalar p and any 3-vector $\boldsymbol{q}$, the quaternion $\mathfrak{q} = [p, \boldsymbol{q}]$ is defined as (Gothic fonts denote quaternions)

$$\mathfrak{q} = [p, \boldsymbol{q}] = pI - \sum_{i=1}^{3} q_i \sigma_i, \tag{1.14}$$

where $\{\sigma_1, \sigma_2, \sigma_3\}$ are the three Pauli spin-matrices defined by

$$\sigma_1 = \begin{pmatrix} 0 & i \\ i & 0 \end{pmatrix}, \qquad \sigma_2 = \begin{pmatrix} 0 & 1 \\ -1 & 0 \end{pmatrix}, \qquad \sigma_3 = \begin{pmatrix} i & 0 \\ 0 & -i \end{pmatrix}, \tag{1.15}$$

I is the 2×2 unit matrix, and $\{\sigma_1, \sigma_2, \sigma_3\}$ obey the relations $\sigma_i \sigma_j = -\delta_{ij} I - \epsilon_{ijk} \sigma_k$. These give the non-commutative multiplication rule

$$\mathfrak{q}_1 \circledast \mathfrak{q}_2 = [p_1 p_2 - \boldsymbol{q}_1 \cdot \boldsymbol{q}_2, p_1 \boldsymbol{q}_2 + p_2 \boldsymbol{q}_1 + \boldsymbol{q}_1 \times \boldsymbol{q}_2]. \tag{1.16}$$

It can easily be demonstrated that quaternions are associative. One of the main properties of quaternions not shared by 3-vectors is the fact that they have an inverse; the inverse of $\mathfrak{q}$ is $\mathfrak{q}^* = [p, -\boldsymbol{q}]$ which means that $\mathfrak{q} \circledast \mathfrak{q}^* = [p^2 + q^2, 0] = (p^2 + q^2)[1, 0]$; of course, $[1, 0]$ really denotes a scalar, so if $p^2 + q^2 = 1$, then $\mathfrak{q}$ is a unit quaternion $\hat{\mathfrak{q}}$.

A quaternion of the type $\mathfrak{w} = [0, \boldsymbol{w}]$ is called a pure quaternion, with the product between two of them expressed as

$$\mathfrak{w}_1 \circledast \mathfrak{w}_2 = [0, \boldsymbol{w}_1] \circledast [0, \boldsymbol{w}_2] = [-\boldsymbol{w}_1 \cdot \boldsymbol{w}_2, \boldsymbol{w}_1 \times \boldsymbol{w}_2]. \tag{1.17}$$

In fact, there is a quaternionic version of the gradient operator $\boldsymbol{\nabla} = [0, \nabla]$, which, when acting upon a pure quaternion $\mathfrak{u} = [0, \boldsymbol{u}]$, gives

$$\boldsymbol{\nabla} \circledast \mathfrak{u} = [-\operatorname{div} \boldsymbol{u}, \operatorname{curl} \boldsymbol{u}]. \tag{1.18}$$

If the field $\boldsymbol{u}$ is divergence-free, as for an incompressible fluid, then

$$\boldsymbol{\nabla} \circledast \mathfrak{u} = [0, \boldsymbol{\omega}]. \tag{1.19}$$

This pure quaternion incorporating the vorticity will be used freely in future sections.

It has been mentioned already in § 1.1 that quaternions are used in the aerospace and computer animation industries to avoid difficulties with Euler angles. Here the relation is briefly sketched between quaternions and one of the many ways that have been used to describe rotating bodies in the rich and long-standing literature of classical mechanics — for more, see [62]. Whittaker [10] shows how quaternions and the *Cayley–Klein parameters* [11] are intimately related and gives explicit formulae relating these parameters to the Euler angles. Let $\hat{\mathfrak{q}} = [p, \boldsymbol{q}]$ be a unit quaternion with inverse $\hat{\mathfrak{q}}^* = [p, -\boldsymbol{q}]$ where $p^2 + q^2 = 1$. For a pure quaternion $\mathfrak{r} = [0, \boldsymbol{r}]$ there exists a transformation $\mathfrak{r} \to \mathfrak{r}' = [0, \boldsymbol{r}']$:

$$\mathfrak{r}' = \hat{\mathfrak{q}} \circledast \mathfrak{r} \circledast \hat{\mathfrak{q}}^*. \tag{1.20}$$

This associative product can be explicitly written as

$$\mathfrak{r}' = \hat{\mathfrak{q}} \circledast \mathfrak{r} \circledast \hat{\mathfrak{q}}^* = \big[0, (p^2 - q^2)\boldsymbol{r} + 2p(\boldsymbol{q} \times \boldsymbol{r}) + 2\boldsymbol{q}(\boldsymbol{r} \cdot \boldsymbol{q})\big]. \tag{1.21}$$

Choosing $p = \pm \cos \frac{1}{2}\theta$ and $\boldsymbol{q} = \pm \hat{\boldsymbol{n}} \sin \frac{1}{2}\theta$, where $\hat{\boldsymbol{n}}$ is the unit normal to $\boldsymbol{r}$, we find that

$$\mathfrak{r}' = \hat{\mathfrak{q}} \circledast \mathfrak{r} \circledast \hat{\mathfrak{q}}^* = \big[0, \boldsymbol{r} \cos\theta + (\hat{\boldsymbol{n}} \times \boldsymbol{r}) \sin\theta\big] \equiv O(\theta, \hat{\boldsymbol{n}})\boldsymbol{r}. \tag{1.22}$$

Equation (1.22) is the Euler–Rodrigues formula for the rotation $O(\theta, \hat{\boldsymbol{n}})$ by an angle θ of the vector $\boldsymbol{r}$ about its unit normal $\hat{\boldsymbol{n}}$; θ and $\hat{\boldsymbol{n}}$ are called the Euler parameters. With the choice of p and $\boldsymbol{q}$ above, $\hat{\mathfrak{q}}$ is given by

$$\hat{\mathfrak{q}} = \pm[\cos \tfrac{1}{2}\theta, \hat{\boldsymbol{n}} \sin \tfrac{1}{2}\theta]. \tag{1.23}$$

The elements of the unit quaternion $\hat{\mathfrak{q}}$ are the Cayley–Klein parameters which are related to the Euler angles and which form a representation of the Lie group $SU(2)$.

All the terms in (1.21) are quadratic in p and $\boldsymbol{q}$, and thus possess the well-known $\pm$-equivalence which is an expression of the fact that $SU(2)$ covers $SO(3)$ twice.[3]

To investigate the map (1.20) when $\hat{\mathfrak{p}}$ is time-dependent, the Euler–Rodrigues formula in (1.22) can be written as

$$\mathfrak{r}'(t) = \hat{\mathfrak{p}} \circledast \mathfrak{r} \circledast \hat{\mathfrak{p}}^* \implies \mathfrak{r} = \hat{\mathfrak{p}}^* \circledast \mathfrak{r}'(t) \circledast \hat{\mathfrak{p}}\,. \tag{1.24}$$

Thus, $\dot{\mathfrak{r}}'$ has a time derivative given by

$$\begin{aligned}\dot{\mathfrak{r}}'(t) &= \dot{\hat{\mathfrak{p}}} \circledast (\hat{\mathfrak{p}}^* \circledast \mathfrak{r}' \circledast \hat{\mathfrak{p}}) \circledast \hat{\mathfrak{p}}^* + \hat{\mathfrak{p}} \circledast (\hat{\mathfrak{p}}^* \circledast \mathfrak{r}' \circledast \hat{\mathfrak{p}}) \circledast \dot{\hat{\mathfrak{p}}}^* \\ &= \dot{\hat{\mathfrak{p}}} \circledast \hat{\mathfrak{p}}^* \circledast \mathfrak{r}' + \mathfrak{r}' \circledast \hat{\mathfrak{p}} \circledast \dot{\hat{\mathfrak{p}}}^* \\ &= (\dot{\hat{\mathfrak{p}}} \circledast \hat{\mathfrak{p}}^*) \circledast \mathfrak{r}' + \mathfrak{r}' \circledast (\dot{\hat{\mathfrak{p}}} \circledast \hat{\mathfrak{p}}^*)^* \\ &= (\dot{\hat{\mathfrak{p}}} \circledast \hat{\mathfrak{p}}^*) \circledast \mathfrak{r}' - ((\dot{\hat{\mathfrak{p}}} \circledast \hat{\mathfrak{p}}^*) \circledast \mathfrak{r}')^*\,,\end{aligned} \tag{1.25}$$

having used the fact on the last line that because $\mathfrak{r}'$ is a pure quaternion, $\mathfrak{r}'^* = -\mathfrak{r}'$. Because $\hat{\mathfrak{p}} = [p, \boldsymbol{q}]$ is of unit length, and thus $p\dot{p} + q\dot{q} = 0$, this means that $\dot{\hat{\mathfrak{p}}} \circledast \hat{\mathfrak{p}}^*$ is also a pure quaternion

$$\dot{\hat{\mathfrak{p}}} \circledast \hat{\mathfrak{p}}^* = [0, \tfrac{1}{2}\boldsymbol{\Omega}_0(t)]\,. \tag{1.26}$$

The 3-vector entry in (1.26) defines the angular frequency $\boldsymbol{\Omega}_0(t)$ as $\boldsymbol{\Omega}_0 = 2(-\dot{p}\boldsymbol{q} + \dot{\boldsymbol{q}}p - \dot{\boldsymbol{q}} \times \boldsymbol{q})$ thereby giving the well-known formula for the rotation of a rigid body

$$\dot{\boldsymbol{r}}' = \boldsymbol{\Omega}_0 \times \boldsymbol{r}'\,. \tag{1.27}$$

For a Lagrangian particle, the equivalent of $\boldsymbol{\Omega}_0$ is the Darboux vector $\boldsymbol{\mathcal{D}}_a$ in Theorem 1 of § 2. This theorem is the main result of this paper and is the equivalent of (1.27) for a Lagrangian particle undergoing rotation in flight.

Finally, it can easily be seen that Hamilton's relation in terms of hyper-complex numbers $i^2 = j^2 = k^2 = ijk = -1$ will generate the rule in (1.16) if $\mathfrak{q}$ is written as a 4-vector $\mathfrak{q} = p + iq_1 + jq_2 + kq_3$. Sudbery's paper [60] is still the best source for a study of the functional properties of quaternions; he discusses how various results familiar for functions over a complex field, such as the Cauchy–Riemann equations, Cauchy's Theorem and integral formula, together with the Laurent expansion (but not conformal maps) have their parallels for quaternionic functions. More recent work on further analytical properties can be found in [61].

2. Lagrangian evolution equations and an orthonormal frame

This section sets up the mathematical foundation concerning the association of quaternion frames and can be found in the paper by Gibbon and Holm [62]. Let us repeat the Lagrangian evolution equations for a vector field $\boldsymbol{w}$ satisfying (1.7) and (1.8)

$$\frac{D\boldsymbol{w}}{Dt} = \boldsymbol{a}(\boldsymbol{x}, t), \qquad \frac{D\boldsymbol{a}}{Dt} = \boldsymbol{b}(\boldsymbol{x}, t). \tag{2.1}$$

[3] *Editor's note*: The next paragraph was inadvertently omitted from the paper in *Uspekhi Mat. Nauk* and has been included in the English translation.

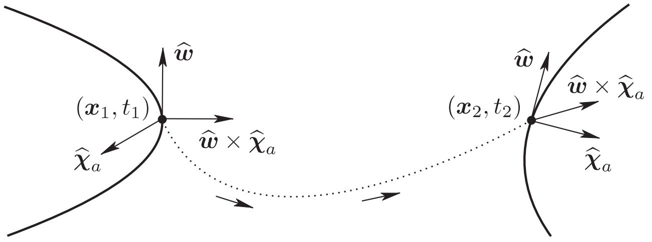

Figure 1. The dotted line represents the tracer particle (•) path moving from $(\boldsymbol{x}_1, t_1)$ to $(\boldsymbol{x}_2, t_2)$. The solid curves represent characteristic curves $\boldsymbol{w} = d\boldsymbol{x}/ds$ to which $\widehat{\boldsymbol{w}}$ is a unit tangent vector. The orientation of the quaternion-frame $(\widehat{\boldsymbol{w}}, \widehat{\boldsymbol{\chi}}_a, \widehat{\boldsymbol{w}} \times \widehat{\boldsymbol{\chi}}_a)$ is shown at the two space-time points; note that this is not the Frenet-frame corresponding to the particle path but to the characteristic curves $\boldsymbol{w}$.

Given the Lagrangian equations in (2.1), define the scalar α_a and the 3-vector $\boldsymbol{\chi}_a$ as[4]

$$\alpha_a = |\boldsymbol{w}|^{-1}(\widehat{\boldsymbol{w}} \cdot \boldsymbol{a}), \qquad \boldsymbol{\chi}_a = |\boldsymbol{w}|^{-1}(\widehat{\boldsymbol{w}} \times \boldsymbol{a}), \qquad \boldsymbol{w} \neq 0. \tag{2.2}$$

Moreover, let α_b and $\boldsymbol{\chi}_b$ be defined as in (2.2) for α_a and $\boldsymbol{\chi}_a$ with $\boldsymbol{a}$ replaced by $\boldsymbol{b}$. The 3-vector $\boldsymbol{a}$ can be decomposed into parts that are parallel and perpendicular to $\boldsymbol{w}$ (and the same for $\boldsymbol{b}$):

$$\boldsymbol{a} = \alpha_a \boldsymbol{w} + \boldsymbol{\chi}_a \times \boldsymbol{w} = [\alpha_a, \boldsymbol{\chi}_a] \circledast [0, \boldsymbol{w}], \tag{2.3}$$

and thus the quaternionic product is summoned in a natural manner. By definition, the growth rate α_a of the magnitude $|\boldsymbol{w}|$ obeys

$$\frac{D|\boldsymbol{w}|}{Dt} = \alpha_a |\boldsymbol{w}|, \tag{2.4}$$

while the unit tangent vector $\widehat{\boldsymbol{w}} = \boldsymbol{w} w^{-1}$ satisfies

$$\frac{D\widehat{\boldsymbol{w}}}{Dt} = \boldsymbol{\chi}_a \times \widehat{\boldsymbol{w}}. \tag{2.5}$$

Now identify the quaternions[5]

$$\mathfrak{q}_a = [\alpha_a, \boldsymbol{\chi}_a], \qquad \mathfrak{q}_b = [\alpha_b, \boldsymbol{\chi}_b], \tag{2.6}$$

and let $\mathfrak{w} = [0, \boldsymbol{w}]$ be the pure quaternion satisfying the Lagrangian evolution equation (2.1). Then the first equation in (2.1) can automatically be re-written equivalently in the quaternion form

$$\frac{D\mathfrak{w}}{Dt} = [0, \boldsymbol{a}] = [0, \alpha_a \boldsymbol{w} + \boldsymbol{\chi}_a \times \boldsymbol{w}] = \mathfrak{q}_a \circledast \mathfrak{w}. \tag{2.7}$$

[4]The role of null points $\boldsymbol{w} = 0$ is not yet clear, although, as § 3 shows, this problem is neatly avoided by the Euler fluid equations. It has been discussed at greater length in [62].

[5]Dropping the a, b labels and normalizing, the Cayley–Klein parameters are $\hat{\mathfrak{q}} = [\alpha, \boldsymbol{\chi}](\alpha^2 + \chi^2)^{-1/2}$.

Moreover, if $\boldsymbol{a}$ is differentiable in the Lagrangian sense as in (2.1), then it is clear that a similar decomposition for $\boldsymbol{b}$ as that for $\boldsymbol{a}$ in (2.3) gives

$$\frac{D^2\mathfrak{w}}{Dt^2} = [0, \boldsymbol{b}] = [0, \alpha_b\boldsymbol{w} + \boldsymbol{\chi}_b \times \boldsymbol{w}] = \mathfrak{q}_b \circledast \mathfrak{w}. \tag{2.8}$$

By using the associativity property, the compatibility of (2.8) and (2.7) implies that (provided $|\boldsymbol{w}| \neq 0$)

$$\left(\frac{D\mathfrak{q}_a}{Dt} + \mathfrak{q}_a \circledast \mathfrak{q}_a - \mathfrak{q}_b\right) \circledast \mathfrak{w} = 0, \tag{2.9}$$

which establishes a *Riccati relation* between $\mathfrak{q}_a$ and $\mathfrak{q}_b$:

$$\frac{D\mathfrak{q}_a}{Dt} + \mathfrak{q}_a \circledast \mathfrak{q}_a = \mathfrak{q}_b. \tag{2.10}$$

This relation is closely allied to the orthonormal quaternion-frame[6] $(\widehat{\boldsymbol{w}}, \widehat{\boldsymbol{\chi}}_a, \widehat{\boldsymbol{w}} \times \widehat{\boldsymbol{\chi}}_a)$ whose equations of motion are given as follows.

Theorem 1 [62]**.** *For the system of equations* (2.1) *relating the* 3*-vectors* $\boldsymbol{w}$, $\boldsymbol{a}$, *and* $\boldsymbol{b}$, *the orthonormal quaternion-frame* $(\widehat{\boldsymbol{w}}, \widehat{\boldsymbol{\chi}}_a, \widehat{\boldsymbol{w}} \times \widehat{\boldsymbol{\chi}}_a) \in SO(3)$ *has Lagrangian time derivatives expressed as*

$$\frac{D\widehat{\boldsymbol{w}}}{Dt} = \boldsymbol{\mathcal{D}}_{ab} \times \widehat{\boldsymbol{w}}, \tag{2.11}$$

$$\frac{D(\widehat{\boldsymbol{w}} \times \widehat{\boldsymbol{\chi}}_a)}{Dt} = \boldsymbol{\mathcal{D}}_{ab} \times (\widehat{\boldsymbol{w}} \times \widehat{\boldsymbol{\chi}}_a), \tag{2.12}$$

$$\frac{D\widehat{\boldsymbol{\chi}}_a}{Dt} = \boldsymbol{\mathcal{D}}_{ab} \times \widehat{\boldsymbol{\chi}}_a, \tag{2.13}$$

where the Darboux angular velocity vector $\boldsymbol{\mathcal{D}}_{ab}$ *is defined as*

$$\boldsymbol{\mathcal{D}}_{ab} = \boldsymbol{\chi}_a + \frac{c_b}{\chi_a}\widehat{\boldsymbol{w}}, \qquad c_b = \widehat{\boldsymbol{w}} \cdot (\widehat{\boldsymbol{\chi}}_a \times \boldsymbol{\chi}_b), \tag{2.14}$$

$\boldsymbol{\chi}_a$ *is defined in* (2.2), *and likewise* $\boldsymbol{\chi}_b$.

Remark. The analogy with the formula for a rigid body is obvious when compared to (1.27), but the Darboux angular velocity $\boldsymbol{\mathcal{D}}_{ab}$ is itself a function of $\boldsymbol{\chi}$, $\widehat{\boldsymbol{w}}$, and other variables and sits in a two-dimensional plane. In turn this is driven by $c_b = \widehat{\boldsymbol{w}} \cdot (\widehat{\boldsymbol{\chi}}_a \times \boldsymbol{\chi}_b)$, for which $\boldsymbol{b}$ must be known. Given this, it may then be possible to numerically solve equations (2.11)–(2.14) for the particle paths.

Proof. To find an expression for the Lagrangian time derivatives of the components of the frame $(\widehat{\boldsymbol{w}}, \widehat{\boldsymbol{\chi}}_a, \widehat{\boldsymbol{w}} \times \widehat{\boldsymbol{\chi}}_a)$ requires the derivative of $\widehat{\boldsymbol{\chi}}_a$. To find this it is necessary to use the fact that the 3-vector $\boldsymbol{b}$ can be expressed in this orthonormal frame as the linear combination

$$w^{-1}\boldsymbol{b} = \alpha_b\widehat{\boldsymbol{w}} + c_b\widehat{\boldsymbol{\chi}}_a + d_b(\widehat{\boldsymbol{w}} \times \widehat{\boldsymbol{\chi}}_a), \tag{2.15}$$

[6] According to Hanson [2] the quaternion-frame is similar to the Bishop-frame in computer graphics.

where c_b is defined in (2.14) and $d_b = -(\widehat{\boldsymbol{\chi}}_a \cdot \boldsymbol{\chi}_b)$. The 3-vector product $\boldsymbol{\chi}_b = w^{-1}(\widehat{\boldsymbol{w}} \times \boldsymbol{b})$ yields

$$\boldsymbol{\chi}_b = c_b(\widehat{\boldsymbol{w}} \times \widehat{\boldsymbol{\chi}}_a) - d_b\widehat{\boldsymbol{\chi}}_a. \tag{2.16}$$

To find the Lagrangian time derivative of $\widehat{\boldsymbol{\chi}}_a$, we use the 3-vector part of the equation for the quaternion $\mathfrak{q}_a = [\alpha_a, \boldsymbol{\chi}_a]$ in Theorem 1:

$$\frac{D\boldsymbol{\chi}_a}{Dt} = -2\alpha_a\boldsymbol{\chi}_a + \boldsymbol{\chi}_b \implies \frac{D\chi_a}{Dt} = -2\alpha_a\chi_a - d_b, \tag{2.17}$$

where $\chi_a = |\boldsymbol{\chi}_a|$. By (2.16) and (2.17) there follows

$$\frac{D\widehat{\boldsymbol{\chi}}_a}{Dt} = c_b\chi_a^{-1}(\widehat{\boldsymbol{w}} \times \widehat{\boldsymbol{\chi}}_a), \qquad \frac{D(\widehat{\boldsymbol{w}} \times \widehat{\boldsymbol{\chi}}_a)}{Dt} = \chi_a\widehat{\boldsymbol{w}} - c_b\chi_a^{-1}\widehat{\boldsymbol{\chi}}_a, \tag{2.18}$$

which gives equations (2.11)–(2.14). This proves Theorem 1.

How to find the rate of change of acceleration represented by the $\boldsymbol{b}$-vector is an important question regarding computing the paths of passive tracer particles when $\boldsymbol{b}$ is not known through Ertel's theorem. The result that follows describes the evolution of $\mathfrak{q}_b$ in terms of three arbitrary scalars.

Theorem 2 [62]**.** *The Lagrangian time derivative of* $\mathfrak{q}_b$ *can be expressed as*

$$\frac{D\mathfrak{q}_b}{Dt} = \mathfrak{q}_a \circledast \mathfrak{q}_b + \lambda_1\mathfrak{q}_b + \lambda_2\mathfrak{q}_a + \lambda_3\mathbb{I}, \tag{2.19}$$

where the $\lambda_i = \lambda_i(\boldsymbol{x}, t)$ *are arbitrary scalars* $\big(\mathbb{I} = [1, 0]\big)$.

Proof. To establish (2.19), we differentiate the orthogonality relation $\boldsymbol{\chi}_b \cdot \widehat{\boldsymbol{w}} = 0$ and use the Lagrangian derivative of $\widehat{\boldsymbol{w}}$:

$$\frac{D\boldsymbol{\chi}_b}{Dt} = \boldsymbol{\chi}_a \times \boldsymbol{\chi}_b + \boldsymbol{s}_0, \qquad \text{where} \qquad \boldsymbol{s}_0 = \mu\boldsymbol{\chi}_a + \lambda\boldsymbol{\chi}_b. \tag{2.20}$$

The vector $\boldsymbol{s}_0$ lies in the plane perpendicular to $\widehat{\boldsymbol{w}}$ in which $\boldsymbol{\chi}_a$ and $\boldsymbol{\chi}_b$ also lie, and $\mu = \mu(\boldsymbol{x}, t)$ and $\lambda = \lambda(\boldsymbol{x}, t)$ are arbitrary scalars. Explicitly differentiating $\boldsymbol{\chi}_b = w^{-1}(\widehat{\boldsymbol{w}} \times \boldsymbol{b})$ gives

$$w^{-1}\widehat{\boldsymbol{w}}(\boldsymbol{\chi}_a \cdot \boldsymbol{b}) + \boldsymbol{s}_0 = -\alpha_a\boldsymbol{\chi}_b - \alpha_b\boldsymbol{\chi}_a + w^{-1}\widehat{\boldsymbol{w}}(\boldsymbol{\chi}_a \cdot \boldsymbol{b}) + w^{-1}\left(\widehat{\boldsymbol{w}} \times \frac{D\boldsymbol{b}}{Dt}\right), \tag{2.21}$$

which can easily be manipulated into

$$\widehat{\boldsymbol{w}} \times \left\{\frac{D\boldsymbol{b}}{Dt} - \alpha_b\boldsymbol{a} - \alpha_a\boldsymbol{b}\right\} = w\boldsymbol{s}_0. \tag{2.22}$$

This means that

$$\frac{D\boldsymbol{b}}{Dt} = \alpha_b\boldsymbol{a} + \alpha_a\boldsymbol{b} + \boldsymbol{s}_0 \times \boldsymbol{w} + \varepsilon\boldsymbol{w}, \tag{2.23}$$

where $\varepsilon = \varepsilon(\boldsymbol{x}, t)$ is a third unknown scalar in addition to μ and λ in (2.20). Thus, the Lagrangian derivative of $\alpha_b = w^{-1}(\widehat{\boldsymbol{w}} \cdot \boldsymbol{b})$ is

$$\frac{D\alpha_b}{Dt} = \alpha\alpha_b + \boldsymbol{\chi}_a \cdot \boldsymbol{\chi}_b + \varepsilon. \tag{2.24}$$

Lagrangian differential relations have now been found for $\boldsymbol{\chi}_b$ and α_b, but at the price of introducing the triplet of unknown coefficients μ, λ, and ε, which can be re-defined as

$$\lambda = \alpha_a + \lambda_1, \qquad \mu = \alpha_b + \lambda_2, \qquad \varepsilon = -2\boldsymbol{\chi}_a \cdot \boldsymbol{\chi}_b + \lambda_2\alpha_a + \lambda_1\alpha_b + \lambda_3. \tag{2.25}$$

The new triplet has been subsumed into (2.19). Then (2.20) and (2.24) can be written in the quaternion form (2.19). Theorem 2 is proved.

3. Quaternions and the incompressible 3*D* Euler equations

The results of the previous section on Lagrangian flows are immediately applicable to the incompressible Euler equations, but to present them in this manner is actually to do so in the chronologically reverse order in which they were first developed. Looking ahead in this section, we note that the variables α and $\boldsymbol{\chi}$ in (3.4) for the Euler equations, and the two coupled differential equations (3.10) that they satisfy, were first written down almost ten years ago in [63], [64] without the help of quaternions. It was then discovered in [65] that these equations could be combined to form a quaternionic Riccati equation. Finally, the more recent paper [59], in combination with [62], put all these results in the form expounded in this present paper. Because data for the three-dimensional Euler equations gets very rough very quickly, it should be understood that all our manipulations are formal.

In § 2 it was shown that a knowledge of the quartet of vectors $(\boldsymbol{u}, \boldsymbol{w}, \boldsymbol{a}, \boldsymbol{b})$ is necessary to be able to use the results of Theorem 1. With $\boldsymbol{w} \equiv \boldsymbol{\omega}$ and $\boldsymbol{\omega} = \mathrm{curl}\,\boldsymbol{u}$, the vortex stretching vector is $\boldsymbol{a} = \boldsymbol{\omega}\cdot\nabla\boldsymbol{u}$. Thus, the $\boldsymbol{w}$- and $\boldsymbol{u}$-fields are not independent in this case. Within $\boldsymbol{a} = \boldsymbol{\omega}\cdot\nabla\boldsymbol{u}$, the dot-product of $\boldsymbol{\omega}$ sees only the symmetric part of the velocity gradient matrix $\nabla\boldsymbol{u}$, which is the strain matrix $S_{ij} = \frac{1}{2}(u_{i,j} + u_{j,i})$ defined in (1.6). With $\boldsymbol{a} = \boldsymbol{\omega}\cdot\nabla\boldsymbol{u} = S\boldsymbol{\omega}$, the triad of vectors is

$$(\boldsymbol{u}, \boldsymbol{w}, \boldsymbol{a}) \equiv (\boldsymbol{u}, \boldsymbol{\omega}, S\boldsymbol{\omega}). \tag{3.1}$$

To find the $\boldsymbol{b}$-field, Ertel's theorem of § 1.2 comes to the rescue. The derivative $D\boldsymbol{u}/Dt$ within the right-hand side of (1.1) (with $\boldsymbol{w} = \boldsymbol{\omega}$) obeys Euler's equation $D\boldsymbol{u}/Dt = -\nabla p$, so we have

$$\boldsymbol{b} = \boldsymbol{\omega}\cdot\nabla\left(\frac{D\boldsymbol{u}}{Dt}\right) = -P\boldsymbol{\omega}, \tag{3.2}$$

where P is the Hessian of the pressure defined in (1.4). The quartet of vectors necessary to make Theorem 1 work is now in place:

$$(\boldsymbol{u}, \boldsymbol{w}, \boldsymbol{a}, \boldsymbol{b}) \equiv (\boldsymbol{u}, \boldsymbol{\omega}, S\boldsymbol{\omega}, -P\boldsymbol{\omega}). \tag{3.3}$$

Table 1 presents three quartets $(\boldsymbol{u}, \boldsymbol{w}, \boldsymbol{a}, \boldsymbol{b})$ for the Euler fluid equations.

Under the definitions in § 2 the scalar α and the 3-vector $\boldsymbol{\chi}$ are defined as

$$\alpha = \widehat{\boldsymbol{\omega}}\cdot S\widehat{\boldsymbol{\omega}}, \qquad \boldsymbol{\chi} = \widehat{\boldsymbol{\omega}} \times S\widehat{\boldsymbol{\omega}}, \tag{3.4}$$

and α_p and $\boldsymbol{\chi}_p$ as

$$\alpha_p = \widehat{\boldsymbol{\omega}}\cdot P\widehat{\boldsymbol{\omega}}, \qquad \boldsymbol{\chi}_p = \widehat{\boldsymbol{\omega}} \times P\widehat{\boldsymbol{\omega}}. \tag{3.5}$$

Table 1. The entries below are three of the possibilities for finding a $\boldsymbol{b}$-field given the triplet $(\boldsymbol{u},\boldsymbol{w},\boldsymbol{a})$. The third line is the result (3.3), while $\boldsymbol{b}$ is unknown for the second line.

$\boldsymbol{u}$	$\boldsymbol{w}$	$\boldsymbol{a}$	$\boldsymbol{b}$	Material derivative
Euler	$\boldsymbol{x}$	$\boldsymbol{u}$	$-\nabla p$	(1.2)
Euler	$\boldsymbol{u}$	$-\nabla p$	?	(1.2)
Euler	$\boldsymbol{w}$	$S\boldsymbol{w}$	$-P\boldsymbol{w}$	(1.2)

The quantity α in (3.4) is now identified as the same as in Constantin [55], who expressed it as an explicit Biot–Savart formula.[7] The vector $\boldsymbol{a} = S\boldsymbol{\omega}$ can be decomposed into parts that are parallel and perpendicular to $\boldsymbol{\omega}$:

$$S\boldsymbol{\omega} = \alpha\boldsymbol{\omega} + \boldsymbol{\chi}\times\boldsymbol{\omega} = [\alpha,\boldsymbol{\chi}] \circledast [0,\boldsymbol{\omega}]. \tag{3.6}$$

By definition, the growth rate α of the scalar magnitude $|\boldsymbol{\omega}|$ and the unit tangent vector $\widehat{\boldsymbol{\omega}}$ obey

$$\frac{D|\boldsymbol{\omega}|}{Dt} = \alpha|\boldsymbol{\omega}|, \qquad \frac{D\widehat{\boldsymbol{\omega}}}{Dt} = \boldsymbol{\chi}\times\widehat{\boldsymbol{\omega}}, \tag{3.7}$$

which show that α drives the growth or collapse of vorticity and $\boldsymbol{\chi}$ determines the rate of swing of $\widehat{\boldsymbol{\omega}}$ around $S\boldsymbol{\omega}$. Now we identify the quaternions

$$\mathfrak{q} = [\alpha,\boldsymbol{\chi}], \qquad \mathfrak{q}_p = [\alpha_p,\boldsymbol{\chi}_p]. \tag{3.8}$$

The equivalent of the Riccati equation (2.10) is[8]

$$\frac{D\mathfrak{q}}{Dt} + \mathfrak{q}\circledast\mathfrak{q} + \mathfrak{q}_p = 0, \tag{3.9}$$

which, when written explicitly in terms of α and $\boldsymbol{\chi}$, becomes

$$\frac{D\alpha}{Dt} + \alpha^2 - \chi^2 + \alpha_p = 0, \qquad \frac{D\boldsymbol{\chi}}{Dt} + 2\alpha\boldsymbol{\chi} + \boldsymbol{\chi}_p = 0. \tag{3.10}$$

In Theorem 1 we need to use $\boldsymbol{b} = -P\boldsymbol{\omega}$ to calculate the path of the orthonormal quaternion-frame $(\widehat{\boldsymbol{\omega}}, \widehat{\boldsymbol{\chi}}, \widehat{\boldsymbol{\omega}}\times\widehat{\boldsymbol{\chi}})$. Specifically, we must solve

$$\frac{D\widehat{\boldsymbol{\omega}}}{Dt} = \boldsymbol{\mathcal{D}}\times\widehat{\boldsymbol{\omega}}, \tag{3.11}$$

$$\frac{D(\widehat{\boldsymbol{\omega}}\times\widehat{\boldsymbol{\chi}})}{Dt} = \boldsymbol{\mathcal{D}}\times(\widehat{\boldsymbol{\omega}}\times\widehat{\boldsymbol{\chi}}), \tag{3.12}$$

$$\frac{D\widehat{\boldsymbol{\chi}}}{Dt} = \boldsymbol{\mathcal{D}}\times\widehat{\boldsymbol{\chi}}, \tag{3.13}$$

[7] Everywhere in [55], [56], [66], [67] the unit vector of vorticity is designated as ξ, whereas here we use $\widehat{\boldsymbol{\omega}}$.

[8] In principle (3.9) can be linearized to a zero-eigenvalue Schrödinger equation in quaternion form with $\mathfrak{q}_p$ as the potential, although it is not clear how to proceed from that point.

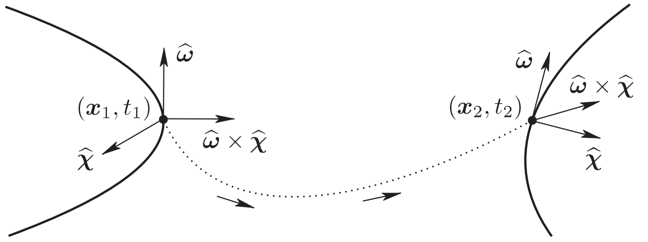

Figure 2. The equivalent of Fig. 1, but for the Euler equations with the dotted line representing an Euler fluid particle (•) path moving from $(\boldsymbol{x}_1, t_1)$ to $(\boldsymbol{x}_2, t_2)$. The solid curves represent vortex lines to which $\widehat{\boldsymbol{\omega}}$ is a unit tangent vector. The orientation of the quaternion-frame $(\widehat{\boldsymbol{\omega}}, \widehat{\boldsymbol{\chi}}, \widehat{\boldsymbol{\omega}} \times \widehat{\boldsymbol{\chi}})$ is shown at the two space-time points; note that this is not the Frenet-frame corresponding to the particle path.

where the Darboux angular velocity vector $\boldsymbol{\mathcal{D}}$ is defined as

$$\boldsymbol{\mathcal{D}} = \boldsymbol{\chi} + \frac{c_p}{\chi}\widehat{\boldsymbol{\omega}}, \qquad c_p = -\widehat{\boldsymbol{\omega}} \cdot (\widehat{\boldsymbol{\chi}} \times \boldsymbol{\chi}_p). \tag{3.14}$$

The pressure Hessian contributes to the angular velocity $\boldsymbol{\mathcal{D}}$ through the scalar coefficient c_p. To compute the fluid particle paths one would need data on the pressure Hessian P as well as the vorticity $\boldsymbol{\omega}$ and the strain matrix S. It is here where the fundamental difference between the Euler equations and a passive problem is made explicit. For the Euler equations the $\boldsymbol{b}$-field containing P is not independent of $\boldsymbol{w} \equiv \boldsymbol{\omega}$ but is connected subtly and non-locally through the elliptic equation for the pressure (1.5), which we repeat here:

$$-\operatorname{Tr} P = \operatorname{Tr} S^2 - \frac{1}{2}\omega^2. \tag{3.15}$$

Theorem 2 expresses the evolution of $\mathfrak{q}_p$,

$$\frac{D\mathfrak{q}_p}{Dt} = \mathfrak{q} \circledast \mathfrak{q}_p + \lambda_1 \mathfrak{q}_p - \lambda_2 \mathfrak{q} - \lambda_3 \mathbb{I}, \tag{3.16}$$

in terms of the arbitrary scalars $\lambda_i(\boldsymbol{x}, t)$. How these can be determined or handled in terms of the incompressibility condition is not clear.

4. The BKM theorem and the direction of vorticity

Three-dimensional Euler data becomes very rough very quickly; thus, understanding how vorticity grows and in what direction, are fundamental questions that have yet to be definitively answered. Clearly, the vortex stretching term $\boldsymbol{\omega} \cdot \nabla \boldsymbol{u} = S\boldsymbol{\omega}$, and the alignment of $\boldsymbol{\omega}$ with the eigenvectors $\boldsymbol{e}_i$ of S, play a fundamental role in determining whether or not a singularity forms in finite time. Major computational studies of this phenomenon can be found in Brachet et al. [68], [69]; Pumir and Siggia [70]; Kerr [71], [72]; Grauer et al. [73]; Boratav and Pelz [74]; Pelz [75]; and Hou and Li [76]. Studies of singularities in the complex time domain of the two-dimensional Euler equations can be found in Pauls, Matsumoto, Frisch, and Bec [77], where an extensive literature is cited.

The BKM theorem [52] is the key result in studying the growth of Euler vorticity and possible singular behaviour. The domain $\mathbb{D} \subset \mathbb{R}^3$ in Theorem 3 is taken to be a three-dimensional periodic domain for present purposes, which guarantees local existence (in time) of classical solutions (Kato [78]), although it is applicable on more general domains than this. One version is (H^s denotes the standard Sobolev space).

Theorem 3 (Beale, Kato, Majda [52]). *On the domain* $\mathbb{D} = [0, L]^3_{\text{per}}$ *there exists a global solution of the Euler equations,* $\boldsymbol{u} \in C\big([0,\infty]; H^s\big) \cap C^1\big([0,\infty]; H^{s-1}\big)$ *for* $s \geqslant 3$, *if for every* $T > 0$

$$\int_0^T \|\boldsymbol{\omega}\|_{L^\infty(\mathbb{D})}\, d\tau < \infty. \tag{4.1}$$

The result can be stated the opposite way, which is that no singularity can form at T without $\int_0^T \|\boldsymbol{\omega}\|_{L^\infty(\mathbb{D})}\, d\tau = \infty$. Theorem 3 has direct computational consequences. In a hypothetical computational experiment if one finds vorticity growth $\|\boldsymbol{\omega}\|_{L^\infty(\mathbb{D})} \sim (T-t)^{-\gamma}$ for some $\gamma > 0$, then the theorem says that γ must satisfy $\gamma \geqslant 1$ for the observed singular behaviour to be real and not an artefact of the numerical computations. The reason is that if γ is found to lie in the range $0 < \gamma < 1$, then $\|\boldsymbol{\omega}\|_{L^\infty(\mathbb{D})}$ blows up whereas its time integral does not, thus violating the theorem. Of the many numerical calculations performed with the Euler equations, that by Kerr [71], [72], using anti-parallel vortex tubes as initial data, was the first to see γ pass the threshold with a critical value of $\gamma = 1$; it was followed by Grauer et al. [73], Boratav and Pelz [74], and Pelz [75]. Recent numerical calculations by Hou and Li [76], however, have contradicted the existence of a singularity: see [79] for a response and a discussion of the issues. To fully settle this question will require more refined computations in tandem with analysis to understand the role played by the direction of vorticity growth. As indicated in § 1, the work of Constantin, Fefferman, and Majda [56] (see also Constantin [55]) was the first to make a precise mathematical formulation of how smooth the direction-of-vortex lines have to be in order to lead to, or prevent, a singularity. § 4.1 is devoted to a short review of this work. Further papers by Cordoba and Fefferman [80], Deng, Hou, and Yu [57], [58], and Chae [66], [67] are variations on this theme. This approach, pioneered in [56], lays the mathematical foundation for the next generation of computational experiments, after the manner of Kerr [71], [72], [79] and Hou and Li [76], to check whether a singularity develops. § 4.2 is devoted to a description of the results in the papers by Deng, Hou, and Yu [57], [58], who have established different criteria on vortex lines. § 4.3 is devoted to an alternative direction-of-vorticity theorem proved in [59], based on the quaternion formulation of this paper.

References and a more global perspective on the Euler equations can be found in the book by Majda and Bertozzi [15]. Shnirelman [81] has constructed very weak solutions (not of Leray type) which have some realistic features but whose kinetic energy monotonically decreases in time and which are everywhere discontinuous and unbounded; for their dynamics in the more exotic function spaces see the papers by Tadmor [82] and Chae [83]–[85].

4.1. The work of Constantin, Fefferman, and Majda. The obvious question regarding the BKM criterion is whether the L^∞-norm can be weakened to L^p for some $1 \leqslant p \leqslant \infty$. This question was addressed by Constantin [55], who placed further assumptions on the local nature of the vorticity and velocity fields. Let us consider the velocity field

$$U_1(t) := \sup_{\boldsymbol{x}} \big|\boldsymbol{u}(\boldsymbol{x},t)\big| \tag{4.2}$$

and the $L^1_{\rm loc}$-norm of $\boldsymbol{\omega}$ defined by

$$\|\boldsymbol{\omega}\|_{1,\rm loc} = L^{-3} \sup_{\boldsymbol{x}} \int_{|\boldsymbol{y}|\leqslant L} \big|\boldsymbol{\omega}(\boldsymbol{x}+\boldsymbol{y})\big|\, d^3y, \tag{4.3}$$

where L is some outer length scale in the Euler flow which could be taken to be unity. Now assume that the unit vector of vorticity is Lipschitz:

$$\big|\widehat{\boldsymbol{\omega}}(\boldsymbol{x},t) - \widehat{\boldsymbol{\omega}}(\boldsymbol{y},t)\big| \leqslant \frac{|\boldsymbol{x}-\boldsymbol{y}|}{\rho_0(t)}, \tag{4.4}$$

for $|\boldsymbol{x}-\boldsymbol{y}| \leqslant L$ and for some length $\rho_0(t)$. Then the following result is stated in Constantin [55] and re-stated and proved in Constantin, Fefferman, and Majda [56].

Theorem 4 (Constantin [55], Constantin, Fefferman, Majda [56]). *Assume that the initial vorticity $\boldsymbol{\omega}_0$ is smooth and compactly supported and assume that a solution of the Euler equations satisfies*

$$\int_0^T \big\|\boldsymbol{\omega}(\cdot,s)\big\|_{1,\rm loc}\left(\frac{L}{\rho_0(s)}\right)^3 ds < \infty, \qquad \int_0^T \frac{U(s)}{\rho_0(s)}\, ds < \infty. \tag{4.5}$$

Then

$$\sup_{0\leqslant t\leqslant T} \frac{\big\|\boldsymbol{\omega}(\cdot,t)\big\|_\infty}{\big\|\boldsymbol{\omega}(\cdot,t)\big\|_{1,\rm loc}} < \infty. \tag{4.6}$$

Clearly, if $U_1 = \|\boldsymbol{u}\|_\infty < \infty$ and $\big\|\boldsymbol{\omega}(\cdot,t)\big\|_{1,\rm loc} < \infty$ on $[0,T]$ and ρ_0 is bounded away from zero, then the BKM theorem says that no singularities can arise. The Lipschitz condition (4.4) can be re-expressed to account for anti-parallel vortex tubes [55].

Constantin, Fefferman, and Majda [56] then considered in more detail how to define the term 'smoothly directed' for trajectories. Consider the three-dimensional Euler equations with smooth localized initial data; assume the solution is smooth on $0 \leqslant t < T$. The velocity field defines particle trajectories $\boldsymbol{X}(\boldsymbol{x}_0,t)$ that satisfy

$$\frac{D\boldsymbol{X}}{Dt} = \boldsymbol{u}(\boldsymbol{X},t), \qquad \boldsymbol{X}(\boldsymbol{x}_0,0) = \boldsymbol{x}_0. \tag{4.7}$$

The image $\boldsymbol{W}_t$ of a set $\boldsymbol{W}_0$ is given by $\boldsymbol{W}_t = \boldsymbol{X}(t,\boldsymbol{W}_0)$. Then the set $\boldsymbol{W}_0$ is said to be *smoothly directed* if there exist a length $\rho > 0$ and a ball of radius $0 < r < \frac{1}{2}\rho$ such that the following three conditions are satisfied.

1. For every $\boldsymbol{x}_0 \in \boldsymbol{W}_0^*$, where $\boldsymbol{W}_0^* = \big\{\boldsymbol{x}_0 \in \boldsymbol{W}_0^*; \big|\boldsymbol{\omega}_0(\boldsymbol{x}_0)\big| \neq 0\big\}$, and all $t \in [0,T)$ the function $\widehat{\boldsymbol{\omega}}(\cdot,t)$ has a Lipschitz extension to the ball $B_{4\rho}$ of radius 4ρ centred

at $\boldsymbol{X}(\boldsymbol{x}_0, t)$, and

$$M = \lim_{t\to T} \sup_{\boldsymbol{x}_0 \in \boldsymbol{W}_0^*} \int_0^t \big\|\nabla \widehat{\boldsymbol{\omega}}(\cdot, s)\big\|^2_{L^\infty(B_{4\rho})}\, ds < \infty. \tag{4.8}$$

This assumption ensures that the direction of vorticity is well-behaved in a neighbourhood of a set of trajectories.

2. The condition

$$\sup_{B_{3r}(\boldsymbol{W}_t)} \big|\boldsymbol{\omega}(\boldsymbol{x}, t)\big| \leqslant m \sup_{B_r(\boldsymbol{W}_t)} \big|\boldsymbol{\omega}(\boldsymbol{x}, t)\big| \tag{4.9}$$

holds for all $t \in [0, T)$ with $m = \text{const} > 0$. This simply means that the chosen neighbourhood captures large and growing vorticity, but not so much that it overlaps with another similar region.

3. The velocity field in the ball of radius 4ρ satisfies

$$\sup_{B_{4r}(\boldsymbol{W}_t)} \big|\boldsymbol{u}(\boldsymbol{x}, t)\big| \leqslant U(t) := \sup_{\boldsymbol{x}} \big|\boldsymbol{u}(\boldsymbol{x}, t)\big| < \infty \tag{4.10}$$

for all $t \in [0, T)$.

Theorem 5 (Constantin, Fefferman, Majda [56]). *Assume that $\boldsymbol{W}_0$ is smoothly directed as in* 1–3 *above. Then there exist a time $\tau > 0$ and a constant Γ such that*

$$\sup_{B_r(\boldsymbol{W}_t)} \big|\boldsymbol{\omega}(\boldsymbol{x}, t)\big| \leqslant \Gamma \sup_{B_\rho(\boldsymbol{W}_t)} \big|\boldsymbol{\omega}(\boldsymbol{x}, t_0)\big| \tag{4.11}$$

holds for any $0 \leqslant t_0 < T$ and $0 \leqslant t - t_0 \leqslant \tau$.

Condition 2 may have implications for how the natural length ρ scales with time as the flow develops [72], but more work needs to be done to understand its implications. Cordoba and Fefferman [80] have weakened condition 3 in the case of vortex tubes to

$$\int_0^T U(s)\, ds = \int_0^T \big\|\boldsymbol{u}(\cdot, s)\big\|_\infty\, ds < \infty. \tag{4.12}$$

4.2. The work of Deng, Hou, and Yu. Deng, Hou, and Yu [57] have re-worked probably the most important of the ‘smoothly directed criteria’, namely (4.8), from local control over $\int_0^t \big\|\nabla\widehat{\boldsymbol{\omega}}(\cdot, t)\big\|^2_{L^\infty} dt$ in $0 \leqslant t \leqslant T$ to a condition on the arc-length s between two points s_1 and s_2. The first of their two results is as follows.

Theorem 6 (Deng, Hou, Yu [57]). *Let $\boldsymbol{x}(t)$ be a family of points with $\big|\boldsymbol{\omega}\big(\boldsymbol{x}(t), t\big)\big| \gtrsim \Omega(t) := \|\boldsymbol{\omega}\|_\infty$. Assume that for all $t \in [0, T]$ there is another point $\boldsymbol{y}(t)$ on the same vortex line as $\boldsymbol{x}(t)$ such that the unit vector of vorticity $\widehat{\boldsymbol{\omega}}(\boldsymbol{x}, t)$ along the line between $\boldsymbol{x}(t)$ and $\boldsymbol{y}(t)$ is well-defined. If it is further assumed that*

$$\left|\int_{s_1}^{s_2} \operatorname{div} \widehat{\boldsymbol{\omega}}(s, t)\, ds\right| \leqslant C(T) \tag{4.13}$$

together with

$$\int_0^T \big|\boldsymbol{\omega}\big(\boldsymbol{x}(t), t\big)\big|\, dt < \infty, \tag{4.14}$$

then there will be no blow-up up to time T. Moreover,

$$e^{-C} \leqslant \frac{\left|\boldsymbol{\omega}\left(\boldsymbol{x}(t),t\right)\right|}{\left|\boldsymbol{\omega}\left(\boldsymbol{y}(t),t\right)\right|} \leqslant e^{C}. \tag{4.15}$$

The inequality (4.13) is based on the simple fact that

$$0 = \operatorname{div}\boldsymbol{\omega} = |\boldsymbol{\omega}|\operatorname{div}\widehat{\boldsymbol{\omega}} + \widehat{\boldsymbol{\omega}}\cdot\nabla|\boldsymbol{\omega}| = |\boldsymbol{\omega}|\operatorname{div}\widehat{\boldsymbol{\omega}} + \frac{d|\boldsymbol{\omega}|}{ds}, \tag{4.16}$$

where $\widehat{\boldsymbol{\omega}}\cdot\nabla = \dfrac{d}{ds}$ is the arc-length derivative.

The second and more important of the results of Deng, Hou, and Yu [58] is based on considering a family of vortex line segments L_t along which the maximum vorticity is comparable with the maximum vorticity $\Omega(t)$. Denote by $L(t)$ the arc length of L_t, by $\hat{\boldsymbol{n}}$ the unit normal vector, and by κ the curvature of the vortex line. Furthermore, they define

$$U_{\widehat{\omega}}(t) \equiv \max_{\boldsymbol{x},\boldsymbol{y}\in L_t}\left|(\boldsymbol{u}\cdot\widehat{\boldsymbol{\omega}})(\boldsymbol{x},t) - (\boldsymbol{u}\cdot\widehat{\boldsymbol{\omega}})(\boldsymbol{y},t)\right|, \tag{4.17}$$

$$U_n(t) \equiv \max_{L_t}|\boldsymbol{u}\cdot\hat{\boldsymbol{n}}|, \tag{4.18}$$

and

$$M(t) \equiv \max\left(\|\nabla\cdot\widehat{\boldsymbol{\omega}}\|_{L^\infty(L_t)}, \|\kappa\|_{L^\infty(L_t)}\right). \tag{4.19}$$

Theorem 7 (Deng, Hou, Yu [57], [58]). *Let $A, B \in (0,1)$ with $B < 1 - A$, and let C_0 be a positive constant. If*

1) $U_{\widehat{\omega}}(t) + U_n(t) \lesssim (T-t)^{-A}$,
2) $M(t)L(t) \leqslant C_0$, *and*
3) $L(t) \gtrsim (T-t)^{B}$,

then there will be no blow-up up to time T.

In a further related paper Deng, Hou, and Yu [58] have changed the inequality $A + B < 1$ to equality $A + B = 1$ subject to a further weak condition. They also derived some improved geometric scaling conditions which can be applied to the scenario when the velocity blows up at the same time as the vorticity and the rate of blow-up of velocity is proportional to the square root of the vorticity. This is the worst possible blow-up scenario for the velocity field due to Kelvin's circulation theorem.

4.3. The non-constancy of $\boldsymbol{\alpha_p}$ and $\boldsymbol{\chi_p}$: quaternions and the direction of vorticity. The key relation in the quaternionic formulation of the Euler equations is the Riccati equation (3.9) for $\mathfrak{q} = \left[\alpha(x,t), \boldsymbol{\chi}(x,t)\right]$. In terms of α and χ this gives four equations

$$\frac{D\alpha}{Dt} = \chi^2 - \alpha^2 - \alpha_p, \qquad \frac{D\boldsymbol{\chi}}{Dt} = -2\alpha\boldsymbol{\chi} - \boldsymbol{\chi}_p. \tag{4.20}$$

Although apparently a simple set of differential equations driven by $\mathfrak{q}_p = [\alpha_p, \boldsymbol{\chi}_p]$, it is clear that $\mathfrak{q}_p$ is not independent of the solution, because of the pressure constraint

$-\operatorname{Tr} P = u_{i,k}u_{k,i}$. In consequence it is tempting to think of $\mathfrak{q}_p$ as behaving in a constant fashion. This may be true for large regions of an Euler flow but it is certainly not true in the most intense vortical regions where vortex lines have their greatest curvature; in these regions the signs of α_p and of the components of $\boldsymbol{\chi}_p$ may change dramatically [64]. It is because of these potentially violent changes that $\mathfrak{q}_p$ could be considered as a candidate for a further conditional direction-of-vorticity theorem along the lines of those in §§ 4.1 and 4.2. Other work where constraints on P appear is the paper by Chae [67].

The work in [56]–[58] shows that $\nabla\widehat{\boldsymbol{\omega}}$ needs to be controlled in some fashion in local areas where vortex lines have high curvature. In terms of the number of derivatives the Hessian P is on the same level, and it is in terms of P and the variables α_p and $\boldsymbol{\chi}_p$ associated with it that we look for control of Euler solutions. From their definitions, it is easily shown that $\alpha^2 + \chi^2 = |S\widehat{\boldsymbol{\omega}}|^2$ and thus on vortex lines $\alpha = \alpha\big(\boldsymbol{X}(t,\boldsymbol{x}_0),t\big)$ the system (4.20) becomes

$$\frac{d}{dt}|S\widehat{\boldsymbol{\omega}}|^2 = -\alpha|S\widehat{\boldsymbol{\omega}}|^2 + \alpha\alpha_p + \boldsymbol{\chi}\cdot\boldsymbol{\chi}_p. \tag{4.21}$$

Thus, on integration

$$\big|S\widehat{\boldsymbol{\omega}}\big(\boldsymbol{X}(\tau),t\big)\big|^2 = -2\int_0^T e^{\int_0^\tau \alpha(\cdot,t')\,dt' - \int_0^t \alpha(\cdot,t')\,dt'}(\alpha\alpha_p + \boldsymbol{\chi}\cdot\boldsymbol{\chi}_p)\boldsymbol{X}(\cdot,\tau)\,d\tau. \tag{4.22}$$

There are now two alternatives. The first is to apply the Cauchy–Schwarz inequality and use the fact that $\alpha_p^2 + \chi_p^2 = |P\widehat{\boldsymbol{\omega}}|^2$:

$$\big|S\widehat{\boldsymbol{\omega}}\big(\boldsymbol{X}(t,\boldsymbol{x}_0),t\big)\big| \leqslant 2\int_0^T e^{\int_0^\tau \alpha(\cdot,t')\,dt' - \int_0^t \alpha(\cdot,t')\,dt'}\big|P\widehat{\boldsymbol{\omega}}(\cdot,\tau)\big|\,d\tau. \tag{4.23}$$

This is similar to Chae's result (Theorem 5.1 in [67]), which is based on control of the time integral of $\|S\widehat{\boldsymbol{\omega}}\cdot P\widehat{\boldsymbol{\omega}}\|_\infty$, which is derivable from (3.2).

The second raises an interesting case respecting the direction of vorticity using $\boldsymbol{\chi}_p$ and can be viewed as an alternative way of looking at the direction of vorticity after [56]–[58]. The vector $\boldsymbol{\chi}_p = \widehat{\boldsymbol{\omega}}\times P\widehat{\boldsymbol{\omega}}$ contains $\widehat{\boldsymbol{\omega}}$ and not $\boldsymbol{\omega}$ and is thus concerned with the direction of $\boldsymbol{\omega}$ rather than its magnitude. Firstly we use the fact that $|\boldsymbol{\omega}|$ cannot blow-up for $\alpha < 0$, because $D|\boldsymbol{\omega}|/Dt = \alpha|\boldsymbol{\omega}|$; thus, our concern is with $\alpha \geqslant 0$. In the case when the angle between $\widehat{\boldsymbol{\omega}}$ and $P\widehat{\boldsymbol{\omega}}$ is not zero,

$$\big|S\widehat{\boldsymbol{\omega}}\big(\boldsymbol{X}(t,\boldsymbol{x}_0),t\big)\big| \leqslant 2\int_0^T \big|\boldsymbol{\chi}_p(\cdot,\tau)\big|\,d\tau. \tag{4.24}$$

If the right-hand side is bounded, then the solution of the Euler equation cannot blow up, excepting the possibility that $|P\widehat{\boldsymbol{\omega}}|$ blows up simultaneously as the angle between $\widehat{\boldsymbol{\omega}}$ and $P\widehat{\boldsymbol{\omega}}$ approaches zero while keeping $\boldsymbol{\chi}_p$ finite; under these circumstances $\int_0^t |\boldsymbol{\chi}_p|\,d\tau < \infty$, whereas $\int_0^t |\alpha_p|\,d\tau \to \infty$, and thus blow-up is still theoretically possible in that case. The result does not imply that blow-up occurs when collinearity does, but rather simply implies that under the condition (4.24) it is the only situation when that can happen. Ohkitani [36] and Ohkitani and

Kishiba [40] have noted the collinearity mentioned above; they observed in Euler computations that at maximum points of enstrophy $\boldsymbol{\omega}$ tends to align with the eigenvector corresponding to the most negative eigenvalue of P. Expressed over the whole periodic volume we have the following theorem.

Theorem 8 (Gibbon, Holm, Kerr, Roulstone [59]). *On the domain $\mathbb{D} = [0, L]^3_{\text{per}}$ there exists a global solution $\boldsymbol{u} \in C\big([0,\infty]; H^s\big) \cap C^1\big([0,\infty]; H^{s-1}\big)$ of the Euler equations for $s \geqslant 3$ if for every $T > 0$*

$$\int_0^T \|\boldsymbol{\chi}_p\|_{L^\infty(\mathbb{D})}\, d\tau < \infty, \tag{4.25}$$

excepting the case where $\widehat{\boldsymbol{\omega}}$ becomes collinear with an eigenvector of P at time T.

5. A final example: the equations of incompressible ideal MHD

The Lagrangian formulation of § 2 can be applied to many situations, such as the stretching of fluid line-elements, incompressible motion of Euler fluids, and ideal MHD (Majda and Bertozzi [15]). We choose ideal MHD in Elsasser variable form as a final example; another approach to this can be found in [86]. The equations for the fluid and the magnetic field $\boldsymbol{B}$ are

$$\frac{D\boldsymbol{u}}{Dt} = \boldsymbol{B}\cdot\nabla\boldsymbol{B} - \nabla p, \tag{5.1}$$

$$\frac{D\boldsymbol{B}}{Dt} = \boldsymbol{B}\cdot\nabla\boldsymbol{u} \tag{5.2}$$

together with $\operatorname{div}\boldsymbol{u} = 0$ and $\operatorname{div}\boldsymbol{B} = 0$. The pressure p in (5.1) is $p_f + \frac{1}{2}B^2$ where p_f is the fluid pressure. Elsasser variables are defined by the combination [30]

$$\boldsymbol{v}^\pm = \boldsymbol{u} \pm \boldsymbol{B}. \tag{5.3}$$

The existence of two velocities $\boldsymbol{v}^\pm$ means that there are two material derivatives

$$\frac{D^\pm}{Dt} = \frac{\partial}{\partial t} + \boldsymbol{v}^\pm\cdot\nabla. \tag{5.4}$$

In terms of these, (5.1) and (5.2) can be rewritten as

$$\frac{D^\pm\boldsymbol{v}^\mp}{Dt} = -\nabla p, \tag{5.5}$$

with the magnetic field $\boldsymbol{B}$ satisfying ($\operatorname{div}\boldsymbol{v}^\pm = 0$)

$$\frac{D^\pm\boldsymbol{B}}{Dt} = \boldsymbol{B}\cdot\nabla\boldsymbol{v}^\pm. \tag{5.6}$$

Thus, we have a pair of triads $(\boldsymbol{v}^\pm, \boldsymbol{B}, \boldsymbol{a}^\pm)$ with $\boldsymbol{a}^\pm = \boldsymbol{B}\cdot\nabla\boldsymbol{v}^\pm$ based on Moffatt's identification of the $\boldsymbol{B}$-field as the important stretching element [30]. From [65], [59] we also have

$$\frac{D^\pm\boldsymbol{a}^\mp}{Dt} = -P\boldsymbol{B}, \tag{5.7}$$

where $\boldsymbol{b}^{\pm} = -P\boldsymbol{B}$. With two quartets $(\boldsymbol{v}^{\pm}, \boldsymbol{B}, \boldsymbol{a}^{\pm}, \boldsymbol{b})$, the results of § 2 follow, with two Lagrangian derivatives and the two Riccati equations

$$\frac{D^{\mp}\mathfrak{q}_a^{\pm}}{Dt} + \mathfrak{q}_a^{\pm} \circledast \mathfrak{q}_a^{\mp} = \mathfrak{q}_b. \tag{5.8}$$

In consequence, MHD-quaternion-frame dynamics needs to be interpreted in terms of two sets of orthonormal frames $(\widehat{\boldsymbol{B}}, \widehat{\boldsymbol{\chi}}^{\pm}, \widehat{\boldsymbol{B}} \times \widehat{\boldsymbol{\chi}}^{\pm})$ acted on by their opposite Lagrangian time derivatives:

$$\frac{D^{\mp}\widehat{\boldsymbol{B}}}{Dt} = \boldsymbol{\mathcal{D}}^{\mp} \times \widehat{\boldsymbol{B}}, \tag{5.9}$$

$$\frac{D^{\mp}}{Dt}(\widehat{\boldsymbol{B}} \times \widehat{\boldsymbol{\chi}}^{\pm}) = \boldsymbol{\mathcal{D}}^{\mp} \times (\widehat{\boldsymbol{B}} \times \widehat{\boldsymbol{\chi}}^{\pm}), \tag{5.10}$$

$$\frac{D^{\mp}\widehat{\boldsymbol{\chi}}^{\pm}}{Dt} = \boldsymbol{\mathcal{D}}^{\mp} \times \widehat{\boldsymbol{\chi}}^{\pm}, \tag{5.11}$$

where the pair of Elsasser–Darboux vectors $\boldsymbol{\mathcal{D}}^{\mp}$ is defined as

$$\boldsymbol{\mathcal{D}}^{\mp} = \boldsymbol{\chi}^{\mp} - \frac{c_B^{\mp}}{\chi^{\mp}}\widehat{\boldsymbol{B}}, \qquad c_B^{\mp} = \widehat{\boldsymbol{B}} \cdot \left[\widehat{\boldsymbol{\chi}}^{\pm} \times (\boldsymbol{\chi}_{pB} + \alpha^{\pm}\boldsymbol{\chi}^{\mp})\right]. \tag{5.12}$$

6. Conclusion

The well-established use of quaternions by the aero/astronautics and computer animation communities in the spirit intended by Hamilton gives us confidence that they are applicable to the 'flight' of Lagrangian particles in both passive tracer particle flows and, in particular, three-dimensional Euler flows. An equivalent formulation for the compressible Euler equations [46], [47] may give a clue to the nature of the incompressible limit. This theme will be discussed in a forthcoming paper by the author and H. Esraghi. The case of the barotropic compressible Euler equations and other examples are given in the summary in Table 2.

Table 2. The entries display various examples of the use of Ertel's theorem in closing the quartet of vectors $(\boldsymbol{u}, \boldsymbol{w}, \boldsymbol{a}, \boldsymbol{b})$. For ideal MHD, $D^{\pm}/Dt$ is defined in (5.4).

System	$\boldsymbol{u}$	$\boldsymbol{w}$	$\boldsymbol{a}$	$\boldsymbol{b}$	Material derivative
incompressible Euler	$\boldsymbol{u}$	$\boldsymbol{x}$	$\boldsymbol{u}$	$-\boldsymbol{\nabla} p$	D/Dt
incompressible Euler	$\boldsymbol{u}$	$\boldsymbol{\omega}$	$S\boldsymbol{\omega}$	$-P\boldsymbol{\omega}$	D/Dt
barotropic Euler	$\boldsymbol{u}$	$\boldsymbol{\omega}/\rho$	$\boldsymbol{\omega}/\rho \cdot \boldsymbol{\nabla}\boldsymbol{u}$	$-(\omega_j/\rho)\partial_j(\rho\partial_j p)$	D/Dt
MHD	$\boldsymbol{v}^{\pm}$	$\boldsymbol{B}$	$\boldsymbol{B} \cdot \boldsymbol{\nabla}\boldsymbol{v}^{\mp}$	$-P\boldsymbol{B}$	$D^{\pm}/Dt$
Mixing	$\boldsymbol{u}$	$\boldsymbol{\delta\ell}$	$\boldsymbol{\delta\ell} \cdot \boldsymbol{\nabla}\boldsymbol{u}$	$-P\boldsymbol{\delta\ell}$	D/Dt

Whenever quaternions appear in a natural manner, it is usually a signal that the system has inherent geometric properties. For the Euler equations, it is significant that this entails the growth rate α and the swing rate $\boldsymbol{\chi}$ of the vorticity vector, the latter being very sensitive to the direction of vorticity with respect to eigenvectors of S. To elaborate further, consider a Burgers' vortex which represents a vortex tube [18]. An eigenvector of S lies in the direction of the tube-axis parallel to $\boldsymbol{\omega}$, in which case $\boldsymbol{\chi} = \widehat{\boldsymbol{\omega}} \times S\widehat{\boldsymbol{\omega}} = 0$. However, if a tube comes into close proximity to another, then they will bend and maybe tangle. As soon as the tube-curvature becomes non-zero along a certain line-length, then $\boldsymbol{\chi} \neq 0$ along that length. Likewise, this will also be true for vortex sheets that bend or roll-up when in close proximity to another sheet. The 3-vector $\boldsymbol{\chi}$ is therefore sensitively and locally dependent on the vortical topology. In fact, at each point its evolution is most elegantly expressed through its associated quaternion $\mathfrak{q}$, which must satisfy (see (3.9))

$$\frac{D\mathfrak{q}}{Dt} + \mathfrak{q} \circledast \mathfrak{q} + \mathfrak{q}_p = 0. \tag{6.1}$$

To fully appreciate the power of the method, we note that the pressure field must necessarily appear explicitly in the form of its Hessian through $\mathfrak{q}_p$, although this runs counter to conventional practice in fluid dynamics, where the pressure is usually removed using Leray's projector. The pressure Hessian appears in the material derivative of the vortex stretching term, through the use of Ertel's theorem, as the price to be paid for cancelling the non-linearity $O(|\boldsymbol{\omega}|\,|\nabla \boldsymbol{u}|^2)$. In fact, the effect of the pressure Hessian on the vorticity stretching term is subtle and non-local. Therefore, while it is tempting to discount the pressure because it disappears overtly in the equation for the vorticity, covertly it may arguably be one of the most important terms in inviscid fluid dynamics.

There are, of course, stationary solutions of (6.1), one of which is $\boldsymbol{\chi} = \boldsymbol{\chi}_p = 0$ with $\alpha = \alpha_0$ and $\alpha_p = -\alpha_0^2$. The Burgers' vortex is a solution of this type; see [64], [65]. Having laid much stress in § 4.3 on the non-constancy of α_p and $\boldsymbol{\chi}_p$ in intense, potentially singular regions, let us nevertheless try to determine the simplest generic behaviour of α and $\boldsymbol{\chi}$ from (4.20) when α_p and $\boldsymbol{\chi}_p$ are constant; for example, a near-Burgers' vortex. To do this, let us consider the four equations which come out of (6.1), as in (4.20), and think of them as ordinary differential equations on particle paths $\boldsymbol{X}(t, \boldsymbol{x}_0)$:

$$\dot{\alpha} = \chi^2 - \alpha^2 - \alpha_p, \qquad \dot{\chi} = -2\alpha\boldsymbol{\chi} - C_p. \tag{6.2}$$

In regions of the (α, χ)-phase plane where $\alpha_p = \text{const}$ and $C_p = \widehat{\boldsymbol{\chi}} \cdot \boldsymbol{\chi}_p = \text{const}$, there are two critical points

$$(\alpha, \chi) = (\pm\alpha_0, \chi_0), \qquad 2\alpha_0^2 = \alpha_p + [\alpha_p^2 + C_p^2]^{1/2}. \tag{6.3}$$

Thus, there are two fixed points; one with $\alpha > 0$ (stretching), which is a stable spiral, and one with $\alpha < 0$ (compression); both have a small and equal value of χ_0. The point with $\alpha_0 < 0$ is an unstable spiral, while $\alpha_0 > 0$ is stable. Perhaps it is a surprise that it is the stretching case that is the attracting point, although it should also be noted that these equations without the Hessian terms have arisen in Navier–Stokes turbulence modelling [87].

Finally, the existence of the relation (6.1), and its more general Lagrangian equivalent (3.9), is the key step in proving Theorem 1, from which the frame dynamics is derived. Moreover, for the three-dimensional Euler equations, (6.1) is also the key step in the proof of Theorem 8.

For discussions I would like to thank Darryl Holm, Greg Pavliotis, Trevor Stuart, Arkady Tsinober, and Christos Vassilicos, all of Imperial College London, Uriel Frisch of the Observatoire de Nice, Tom Hou of the California Institute of Technology, Robert Kerr of the University of Warwick, Ian Roulstone of the University of Surrey, Edriss Titi of the Weizmann Institute, Israel and Vladimir Vladimirov of the University of York. For their kind hospitality I would also like to thank the organizers (particularly Professors Andrei Fursikov and Sergei Kuksin) of the Steklov Institute's "Mathematical Hydrodynamics" meeting, held in Moscow in June 2006.

Bibliography

[1] J. J. O'Connor and E. F. Robertson, *Sir William Rowan Hamilton*, `http://www-groups.dcs.st-and.ac.uk/~history/Mathematicians/Hamilton.html`, 1998.

[2] A. J. Hanson, *Visualizing quaternions*, Elsevier, London 2006.

[3] В. И. Арнольд, *Математические методы классической механики*, Наука, Москва 1974; English transl., V. I. Arnol'd, *Mathematical methods of classical mechanics*, Grad. Texts in Math., vol. **60**, Springer-Verlag, New York–Heidelberg 1978.

[4] J. E. Marsden, *Lectures on geometric methods in mathematical physics*, CBMS-NSF Regional Conf. Ser. in Appl. Math., vol. 37, SIAM, Philadelphia 1981.

[5] J. E. Marsden, *Lectures on mechanics*, London Math. Soc. Lecture Note Ser., vol. 174, Cambridge Univ. Press, Cambridge 1992.

[6] A. Cayley, "On certain results being related to quaternions", *Phil. Mag.* **26** (1845), 141–145.

[7] W. R. Hamilton, *Lectures on quaternions*, Cambridge Univ. Press, Cambridge 1853.

[8] W. R. Hamilton, *Elements of quaternions*, Cambridge Univ. Press, Cambridge 1866; *Reprinted*, Chelsea Publ., New York 1969.

[9] P. G. Tait, *An elementary treatise on quaternions*, 3rd ed., Cambridge Univ. Press, Cambridge 1890.

[10] E. T. Whittaker, *A treatise on the analytical dynamics of particles and rigid bodies*, Dover, New York 1944.

[11] F. Klein, *The mathematical theory of the top. Lectures delivered on the occasion of the sesquicentennial celebration of Princeton University*, Dover Phoenix Ed., vol. 2, Dover, Mineola 2004.

[12] J. B. Kuipers, *Quaternions and rotation sequences. A primer with applications to orbits, aerospace, and virtual reality*, Princeton Univ. Press, Princeton 1999.

[13] K. Shoemake, "Animating rotation with quaternion curves", *Comput. Graphics* **19**:3 (1985), 245–254.

[14] V. I. Arnold and B. A. Khesin, *Topological methods in hydrodynamics*, Appl. Math. Sci., vol. 125, Springer-Verlag, New York 1998.

[15] A. J. Majda and A. L. Bertozzi, *Vorticity and incompressible flow*, Cambridge Texts Appl. Math., vol. 27, Cambridge Univ. Press, Cambridge 2002.

[16] G. K. Batchelor, *An introduction to fluid dynamics*, Cambridge Math. Lib., Cambridge Univ. Press, Cambridge 1999.

[17] P. G. Saffman, *Vortex dynamics*, Cambridge Monogr. Mech. Appl. Math., Cambridge Univ. Press, Cambridge 1992.

[18] H. K. Moffatt, S. Kida, and K. Ohkitani, "Stretched vortices — the sinews of turbulence; large-Reynolds-number asymptotics", *J. Fluid Mech.* **259** (1994), 241–264.

[19] A. La Porta, G. A. Voth, A. Crawford, J. Alexander, and E. Bodenschatz, "Fluid particle accelerations in fully developed turbulence", *Nature* **409** (2001), 1017–1019.

[20] N. Mordant, P. Metz, O. Michel, and J.-F. Pinton, "Measurement of Lagrangian velocity in fully developed turbulence", *Phys. Rev. Lett.* **87**:21 (2001), 214501.

[21] G. A. Voth, A. La Porta, A. Crawford, J. Alexander, and E. Bodenschatz, "Measurement of particle accelerations in fully developed turbulence", *J. Fluid Mech.* **469**:1 (2002), 121–160.

[22] N. Mordant, A. M. Crawford, and E. Bodenschatz, "Three-dimensional structure of the Lagrangian acceleration in turbulent flows", *Phys. Rev. Lett.* **93**:21 (2004), 214501.

[23] N. Mordant, E. Lévêque, and J.-F. Pinton, "Experimental and numerical study of the Lagrangian dynamics of high Reynolds turbulence", *New J. Phys.* **6**:1 (2004), 1–116.

[24] N. Mordant, P. Metz, J.-F. Pinton, and O. Michel, "Acoustical technique for Lagrangian velocity measurement", *Rev. Sci. Instrum.* **76**:2 (2005), 025105.

[25] B. A. Lüthi, A. Tsinober, and W. Kinzelbach, "Lagrangian measurement of vorticity dynamics in turbulent flow", *J. Fluid Mech.* **528** (2005), 87–118.

[26] L. Biferale, G. Boffetta, A. Celani, A. Lanotte, and F. Toschi, "Particle trapping in three-dimensional fully developed turbulence", *Phys. Fluids* **17**:2 (2005), 021701.

[27] A. M. Reynolds, N. Mordant, A. M. Crawford, and E. Bodenschatz, "On the distribution of Lagrangian accelerations in turbulent flows", *New J. Phys.* **7** (2005), 58.

[28] W. Braun, F. De Lillo, and B. Eckhardt, "Geometry of particle paths in turbulent flows", *J. Turbul.* **7** (2006), 62.

[29] E. Dresselhaus and M. Tabor, "The kinematics of stretching and alignment of material elements in general flow fields", *J. Fluid Mech.* **236** (1991), 415–444.

[30] H. K. Moffatt, *Magnetic field generation in electrically conducting fluids*, Cambridge Univ. Press, Cambridge 1978.

[31] J. Norbury and I. Roulstone (eds.), *Large-scale atmosphere-ocean dynamics*, vol. 1, 2, Cambridge Univ. Press, Cambridge 2002.

[32] A. J. Majda, *Introduction to PDEs and waves for the atmosphere and ocean*, Courant Lect. Notes Math., vol. 9, Amer. Math. Soc., Providence, RI 2003.

[33] M. J. P. Cullen, *A mathematical theory of large-scale atmosphere/ocean flow*, Imperial College Press, London 2006.

[34] G. Falkovich, K. Gawedzki, and M. Vergassola, "Particles and fields in fluid turbulence", *Rev. Modern Phys.* **73**:4 (2001), 913–975.

[35] H. Ertel, "Ein neuer hydrodynamischer Wirbelsatz", *Meteorolog. Z.* **59** (1942), 277–281.

[36] K. Ohkitani, "Eigenvalue problems in three-dimensional Euler flows", *Phys. Fluids A* **5**:10 (1993), 2570–2572.

[37] В. Е. Захаров, Е. А. Кузнецов, "Гамильтоновский формализм для нелинейных волн", *УФН* **167**:11 (1997), 1137–1167; English transl., V. E. Zakharov and E. A. Kuznetsov, "Hamiltonian formalism for nonlinear waves", *Phys. Usp.* **40**:11 (1997), 1087–1116.

[38] C. Truesdell and R. A. Toupin, "The classical field theories", *Encyclopaedia of physics* (S. Flügge, ed.), vol. 3, part 1, Springer, Berlin 1960, pp. 226–793.

[39] A. Viúdez, "On Ertel's potential vorticity theorem. On the impermeability theorem for potential vorticity", *J. Atmos. Sci.* **56**:4 (1999), 507–516.

[40] K. Ohkitani and S. Kishiba, "Nonlocal nature of vortex stretching in an inviscid fluid", *Phys. Fluids* **7**:2 (1995), 411–421.

[41] В. И. Юдович, "Нестационарные течения идеальной несжимаемой жидкости", *ЖВМиМФ* **3** (1963), 1032–1066; English transl., V. I. Yudovich, "Non-stationary flow of an ideal incompressible liquid", *USSR Comput. Math. and Math. Phys.* **3** (1963), 1407–1456.

[42] О. А. Ладыженская, *Математические вопросы динамики вязкой несжимаемой жидкости*, Физматгиз, Москва 1961; English transl., O. A. Ladyzhenskaya, *The mathematical theory of viscous incompressible flow*, Gordon and Breach, New York 1963.

[43] P. Constantin and C. Foias, *Navier–Stokes equations*, Chicago Lectures in Math., Univ. Chicago Press, Chicago 1988.

[44] C. Foias, O. Manley, R. Rosa, and R. Temam, *Navier–Stokes equations and turbulence*, Encyclopedia Math. Appl., vol. 83, Cambridge Univ. Press, Cambridge 2001.

[45] J. T. Stuart, "Nonlinear Euler partial differential equations: singularities in their solution", *Applied mathematics, fluid mechanics, astrophysics* (Cambridge, MA, USA, 1987) (D. J. Benney, F. H. Shu, and Chi Yuan, eds.), World Sci. Publ., Singapore 1988, pp. 81–95.

[46] J. T. Stuart, "The Lagrangian picture of fluid motion and its implication for flow structures", *IMA J. Appl. Math.* **46**:1–2 (1991), 147–163.

[47] J. T. Stuart, "Singularities in three-dimensional compressible Euler flows with vorticity", *Theoret. Comput. Fluid Dyn.* **10**:1–4 (1998), 385–391.

[48] J. D. Gibbon, A. Fokas, and C. R. Doering, "Dynamically stretched vortices as solutions of the 3D Navier–Stokes equations", *Phys. D* **132**:4 (1999), 497–510.

[49] K. Ohkitani and J. D. Gibbon, "Numerical study of singularity formation in a class of Euler and Navier–Stokes flows", *Phys. Fluids* **12**:12 (2000), 3181–3194.

[50] P. Constantin, "The Euler equations and nonlocal conservative Riccati equations", *Internat. Math. Res. Notices*, 2000, no. 9, 455–465.

[51] J. D. Gibbon, D. R. Moore, and J. T. Stuart, "Exact, infinite energy, blow-up solutions of the three-dimensional Euler equations", *Nonlinearity* **16**:5 (2003), 1823–1831.

[52] J. T. Beale, T. Kato, and A. Majda, "Remarks on the breakdown of smooth solutions for the 3D Euler equations", *Comm. Math. Phys.* **94**:1 (1984), 61–66.

[53] G. Ponce, "Remarks on a paper ['Remarks on the breakdown of smooth solutions for the 3D Euler equations'] by J. T. Beale, T. Kato and A. Majda", *Comm. Math. Phys.* **98**:3 (1985), 349–353.

[54] H. Kozono and Y. Taniuchi, "Limiting case of the Sobolev inequality in BMO, with applications to the Euler equations", *Comm. Math. Phys.* **214**:1 (2000), 191–200.

[55] P. Constantin, "Geometric statistics in turbulence", *SIAM Rev.* **36**:1 (1994), 73–98.

[56] P. Constantin, C. Fefferman, and A. Majda, "Geometric constraints on potentially singular solutions for the 3-D Euler equation", *Comm. Partial Differential Equations* **21**:3–4 (1996), 559–571.

[57] J. Deng, T. Y. Hou, and X. Yu, "Geometric properties and non-blowup of 3D incompressible Euler flow", *Comm. Partial Differential Equations* **30**:1–2 (2005), 225–243.

[58] J. Deng, T. Y. Hou, and X. Yu, "Improved geometric condition for non-blowup of the 3D incompressible Euler equation", *Comm. Partial Differential Equations* **31**:2 (2006), 293–306.

[59] J. D. Gibbon, D. D. Holm, R. M. Kerr, and I. Roulstone, "Quaternions and particle dynamics in Euler fluid flow", *Nonlinearity* **19**:8 (2006), 1969–1983.

[60] A. Sudbery, "Quaternionic analyis", *Math. Proc. Cambridge Philos. Soc.* **85**:2 (1979), 199–225.

[61] A. S. Fokas and D. A. Pinotsis, "Quaternions, evaluation of integrals and boundary value problems", *Comput. Methods Funct. Theory* (to appear).

[62] J. D. Gibbon and D. D. Holm, "Lagrangian particle paths and ortho-normal quaternion frames", *Nonlinearity* **20**:7 (2007), 1745–1759.

[63] B. Galanti, J. D. Gibbon, and M. Heritage, "Vorticity alignment results for the three-dimensional Euler and Navier–Stokes equations", *Nonlinearity* **10**:6 (1997), 1675–1694.

[64] J. D. Gibbon, B. Galanti, and R. M. Kerr, "Stretching and compression of vorticity in the 3D Euler equations", *Turbulence structure and vortex dynamics* (Cambridge, 1999) (J. C. R. Hunt and J. C. Vassilicos, eds.), Cambridge Univ. Press, Cambridge 2000, pp. 23–34.

[65] J. D. Gibbon, "A quaternionic structure in the three-dimensional Euler and ideal magneto-hydrodynamics equation", *Phys. D* **166**:1–2 (2002), 17–28.

[66] D. Chae, "Remarks on the blow-up of the Euler equations and the related equations", *Comm. Math. Phys.* **245**:3 (2004), 539–550.

[67] D. Chae, "On the finite time singularities of the 3D incompressible Euler equations", *Comm. Pure Appl. Math.* **60**:4 (2007), 597–617.

[68] M. E. Brachet, D. I. Meiron, S. A. Orszag, B. G. Nickel, R. H. Morf, and U. Frisch, "Small-scale structure of the Taylor–Green vortex", *J. Fluid Mech.* **130** (1983), 411–452.

[69] M. E. Brachet, V. Meneguzzi, A. Vincent, H. Politano, and P.-L. Sulem, "Numerical evidence of smooth self-similar dynamics and possibility of subsequent collapse for three-dimensional ideal flows", *Phys. Fluids A* **4**:12 (1992), 2845–2854.

[70] A. Pumir and E. Siggia, "Collapsing solutions to the 3-D Euler equations", *Phys. Fluids A* **2**:2 (1990), 220–241.

[71] R. M. Kerr, "Evidence for a singularity of the three-dimensional, incompressible Euler equations", *Phys. Fluids A* **5**:7 (1993), 1725–1746.

[72] R. M. Kerr, "Vorticity and scaling of collapsing Euler vortices", *Phys. Fluids* **17**:7 (2005), 075103.

[73] R. Grauer, C. Marliani, and K. Germaschewski, "Adaptive mesh refinement for singular solutions of the incompressible Euler equations", *Phys. Rev. Lett.* **80**:19 (1998), 4177–4180.

[74] O. N. Boratav and R. B. Pelz, "Direct numerical simulation of transition to turbulence from a high-symmetry initial condition", *Phys. Fluids* **6**:8 (1994), 2757–2784.

[75] R. B. Pelz, "Symmetry and the hydrodynamic blow-up problem", *J. Fluid Mech.* **444** (2001), 299–320.

[76] T. Y. Hou and R. Li, "Dynamic depletion of vortex stretching and non-blowup of the 3-D incompressible Euler equations", *J. Nonlinear Sci.* **16**:6 (2006), 639–664.

[77] W. Pauls, T. Matsumoto, U. Frisch, and J. Bec, "Nature of complex singularities for the 2D Euler equation", *Phys. D* **219**:1 (2006), 40–59.

[78] T. Kato, "Nonstationary flows of viscous and ideal fluids in $\mathbb{R}^3$", *J. Funct. Anal.* **9**:3 (1972), 296–305.

[79] R. M. Kerr, *Computational Euler history*, `arXiv: physics/0607148`, 2006.

[80] D. Cordoba and C. Fefferman, "On the collapse of tubes carried by 3D incompressible flows", *Comm. Math. Phys.* **222**:2 (2001), 293–298.

[81] A. Shnirelman, "On the nonuniqueness of weak solution of the Euler equation", *Comm. Pure Appl. Math.* **50**:12 (1997), 1261–1286.

[82] E. Tadmor, "On a new scale of regularity spaces with applications to Euler's equations", *Nonlinearity* **14**:3 (2001), 513–532.

[83] D. Chae, "On the Euler equations in the critical Triebel–Lizorkin spaces", *Arch. Ration. Mech. Anal.* **170**:3 (2003), 185–210.

[84] D. Chae, "Local existence and blow-up criterion for the Euler equations in the Besov spaces", *Asymptot. Anal.* **38**:3–4 (2004), 339–358.

[85] D. Chae, "Remarks on the blow-up criterion of the three-dimensional Euler equations", *Nonlinearity* **18**:3 (2005), 1021–1029.

[86] J. D. Gibbon and D. D. Holm, *Lagrangian analysis of alignment dynamics for isentropic compressible magnetohydrodynamics*, `arXiv: nlin.CD/0608009`, 2006.

[87] Li Yi and C. Meneveau, "Origin of non-Gaussian statistics in hydrodynamic turbulence", *Phys. Rev. Lett.* **95**:16 (2005), 164502.

J. D. Gibbon
Imperial College London
E-mail: `j.d.gibbon@ic.ac.uk`

Received 27/SEP/06
Translated by J. D. GIBBON